REPORT DOCUMENTATION PAGE

Form Approved OMB NO. 0704-0188

1. REPORT DATE (DD-MM-YYYY)	2. REPORT TYPE	3. DATES COVERED (From - To)
18-10-2012	Final Report	27-Aug-2008 - 26-Aug-2010

4. TITLE AND SUBTITLE
Frequency-Agile Monolithic Ka-Band Filter

5a. CONTRACT NUMBER

5b. GRANT NUMBER
W911NF-08-C-0099

5c. PROGRAM ELEMENT NUMBER
665502

6. AUTHORS
Yongqiang Wang

5d. PROJECT NUMBER

5e. TASK NUMBER

5f. WORK UNIT NUMBER

7. PERFORMING ORGANIZATION NAMES AND ADDRESSES
nGimat Co.
5315 Peachtree Industrial Blvd.

Atlanta, GA 30341 -

8. PERFORMING ORGANIZATION REPORT NUMBER

9. SPONSORING/MONITORING AGENCY NAME(S) AND ADDRESS(ES)
U.S. Army Research Office
P.O. Box 12211
Research Triangle Park, NC 27709-2211

10. SPONSOR/MONITOR'S ACRONYM(S)
ARO

11. SPONSOR/MONITOR'S REPORT NUMBER(S)
54919-PH-ST2.1

12. DISTRIBUTION AVAILIBILITY STATEMENT
Approved for Public Release; Distribution Unlimited

13. SUPPLEMENTARY NOTES
The views, opinions and/or findings contained in this report are those of the author(s) and should not contrued as an official Department of the Army position, policy or decision, unless so designated by other documentation.

14. ABSTRACT
This report was developed under Small Business Technology Transfer Research (STTR) contract for Topic A07-T009, by nGimat and Georgia Tech. In this reporting period, the deposition conditions for BZN and BST thin films were refined, achieved the standard BST composition using a new precursor lot; studied the deposition conditions for tunable BZN thin films; deposited and characterized the BST temperature stable double layer samples; fabricated nGimat designed Ring Ka-band tunable filters and also Georgia Tech designed 2-pole CPW

15. SUBJECT TERMS
STTR report, filter, tunable filter, ferroelectric, ferromagnetic, CCVD, Ka-Band

16. SECURITY CLASSIFICATION OF:			17. LIMITATION OF ABSTRACT	15. NUMBER OF PAGES	19a. NAME OF RESPONSIBLE PERSON
a. REPORT	b. ABSTRACT	c. THIS PAGE			Zhiyong Zhao
UU	UU	UU	UU		19b. TELEPHONE NUMBER 678-287-3944

Report Title

Frequency-Agile Monolithic Ka-Band Filter

ABSTRACT

This report was developed under Small Business Technology Transfer Research (STTR) contract for Topic A07-T009, by nGimat and Georgia Tech. In this reporting period, the deposition conditions for BZN and BST thin films were refined, achieved the standard BST composition using a new precursor lot; studied the deposition conditions for tunable BZN thin films; deposited and characterized the BST temperature stable double layer samples; fabricated nGimat designed Ring Ka-band tunable filters and also Georgia Tech designed 2-pole CPW Kaband tunable filters using new standard BST films.

Enter List of papers submitted or published that acknowledge ARO support from the start of the project to the date of this printing. List the papers, including journal references, in the following categories:

(a) Papers published in peer-reviewed journals (N/A for none)

Received Paper

TOTAL:

Number of Papers published in peer-reviewed journals:

(b) Papers published in non-peer-reviewed journals (N/A for none)

Received Paper

TOTAL:

Number of Papers published in non peer-reviewed journals:

(c) Presentations

Number of Presentations: 0.00

Non Peer-Reviewed Conference Proceeding publications (other than abstracts):

Received Paper

TOTAL:

Number of Non Peer-Reviewed Conference Proceeding publications (other than abstracts):

Peer-Reviewed Conference Proceeding publications (other than abstracts):

Received Paper

TOTAL:

Number of Peer-Reviewed Conference Proceeding publications (other than abstracts):

(d) Manuscripts

Received	Paper

TOTAL:

Number of Manuscripts:

Books

Received	Paper

TOTAL:

Patents Submitted

Patents Awarded

Awards

Graduate Students

NAME	PERCENT_SUPPORTED
FTE Equivalent:	
Total Number:	

Names of Post Doctorates

NAME	PERCENT_SUPPORTED
Stanis Courreges	0.00
Ben Lacroix	0.00
FTE Equivalent:	**0.00**
Total Number:	**2**

Names of Faculty Supported

NAME	PERCENT_SUPPORTED
FTE Equivalent:	
Total Number:	

Names of Under Graduate students supported

NAME	PERCENT SUPPORTED
FTE Equivalent:	
Total Number:	

Student Metrics

This section only applies to graduating undergraduates supported by this agreement in this reporting period

The number of undergraduates funded by this agreement who graduated during this period: .....

The number of undergraduates funded by this agreement who graduated during this period with a degree in science, mathematics, engineering, or technology fields:.....

The number of undergraduates funded by your agreement who graduated during this period and will continue to pursue a graduate or Ph.D. degree in science, mathematics, engineering, or technology fields:.....

Number of graduating undergraduates who achieved a 3.5 GPA to 4.0 (4.0 max scale): .....

Number of graduating undergraduates funded by a DoD funded Center of Excellence grant for Education, Research and Engineering: .....

The number of undergraduates funded by your agreement who graduated during this period and intend to work for the Department of Defense .....

The number of undergraduates funded by your agreement who graduated during this period and will receive scholarships or fellowships for further studies in science, mathematics, engineering or technology fields: .....

Names of Personnel receiving masters degrees

NAME
Total Number:

Names of personnel receiving PHDs

NAME
Total Number:

Names of other research staff

NAME	PERCENT SUPPORTED
FTE Equivalent:	
Total Number:	

Sub Contractors (DD882)

1 a. Georgia Institute of Technology 1 b. 225 NORTH AVENUE

ATLANTA GA 303320357

Sub Contractor Numbers (c):

Patent Clause Number (d-1): 37 CFR 401.14

Patent Date (d-2):

Work Description (e):

Sub Contract Award Date (f-1): 9/1/2008 12:00:00AM

Sub Contract Est Completion Date(f-2): 8/31/2010 12:00:00AM

---

1 a. Georgia Institute of Technology 1 b. 225 NORTH AVENUE

ATLANTA GA 303320357

Sub Contractor Numbers (c):

Patent Clause Number (d-1): 37 CFR 401.14

Patent Date (d-2):

Work Description (e):

Sub Contract Award Date (f-1): 9/1/2008 12:00:00AM

Sub Contract Est Completion Date(f-2): 8/31/2010 12:00:00AM

Inventions (DD882)

Scientific Progress

Technology Transfer

REPORT DOCUMENTATION PAGE

Form Approved
OMB No. 0704-0188

1. REPORT DATE *(DD-MM-YYYY)*	2. REPORT TYPE	3. DATES COVERED *(From - To)*
01/10/2011	Final Report	05/27/10 to 08/26/10

4. TITLE AND SUBTITLE
Frequency-Agile Monolithic Ka-Band Filter

5a. CONTRACT NUMBER
W911NF-08-C-0099

5b. GRANT NUMBER

5c. PROGRAM ELEMENT NUMBER

6. AUTHOR(S)
Yongqiang Wang

5d. PROJECT NUMBER

5e. TASK NUMBER

5f. WORK UNIT NUMBER

7. PERFORMING ORGANIZATION NAME(S) AND ADDRESS(ES)

*n*Gimat, Co.
5315 Peachtree Industrial Blvd.
Chamblee, GA 30341

8. PERFORMING ORGANIZATION REPORT NUMBER

9. SPONSORING / MONITORING AGENCY NAME(S) AND ADDRESS(ES)

Contracting Office
US Army Research Office
RDECOM Acquisition Center-
RTP Division

Monitoring Office
US Army Research Office
P.O. Box 12211
Research Triangle Park,
NC 27709-2211

10. SPONSOR/MONITOR'S ACRONYM(S)
ARO

11. SPONSOR/MONITOR'S REPORT NUMBER(S)

12. DISTRIBUTION / AVAILABILITY STATEMENT
Distribution authorized to U.S. Government agencies only; contains proprietary information, January 15,2011. Other requests for this document shall be referred to US Army Research Office.

13. SUPPLEMENTARY NOTES

14. ABSTRACT
This report was developed under Small Business Technology Transfer Research (STTR) contract for Topic A07-T009, by nGimat and Georgia Tech. In this reporting period, the deposition conditions for BZN and BST thin films were refined, achieved the standard BST composition using a new precursor lot; studied the deposition conditions for tunable BZN thin films; deposited and characterized the BST temperature stable double layer samples; fabricated nGimat designed Ring Ka-band tunable filters and also Georgia Tech designed 2-pole CPW Ka-band tunable filters using new standard BST films.

15. SUBJECT TERMS
STTR report, filter, tunable filter, ferroelectric, ferromagnetic, CCVD, Ka-Band

16. SECURITY CLASSIFICATION OF:			17. LIMITATION OF ABSTRACT	18. NUMBER OF PAGES	19a. NAME OF RESPONSIBLE PERSON
a. REPORT	b. ABSTRACT	c. THIS PAGE			Yongqiang Wang
Unclassified	Unclassified	Unclassified	UL	51	19b. TELEPHONE NUMBER *(include area code)* 770-361-6771

Standard Form 298 (Rev. 8-98)
Prescribed by ANSI Std. 239.18

Frequency-Agile Monolithic Ka-Band Filter

Final Report
(Reporting period: May 27, 2009 – August 26, 2010)

Sponsored by Department of the Army (DOD)
STTR Topic No.: A07-T009
Issued by US ARMY RDECOM ACQ CTR - W911NF
Contract No. W911NF-08-C-0099

Principal Investigator – Yongqiang Wang Ph.D.
*n*Gimat, Co.
5315 Peachtree Industrial Blvd.
Chamblee, GA 30341
(770) 361-6771 (direct)

Effective Date of Contract: August 27, 2008
Contract Expiration Date: August 26, 2010

Government Contacts:

Technical Contract Manager	Contracting Officer
Dr. Marc Ulrich	Leroy R. Hardy
U.S. Army Research Office	U.S. Army Research Office
P.O. Box 12211	RDECOM Acquisition Center-RTP Division
Research Triangle Park, NC 27709-2211	Phone - 919-549-4237
Voice: (919) 549-4319	Fax- 919-549-4388
FAX: (919) 549-4310	leroy.r.hardy@us.army.mil

Final Report

FREQUENCY-AGILE MONOLITHIC KA-BAND FILTER

Contract No. W911NF-08-C-0099

Prepared for

US ARMY RESEARCH OFFICE

For the period

May 27, 2010 – August 26, 2010

Submitted by

Yongqiang Wang, Ph.D. – Principal Investigator (Since 09/01-2009)

TABLE OF CONTENTS

LIST OF FIGURES

LIST OF TABLES

1. Executive Summary

The advances in ferroic thin films make possible frequency-agile monolithic radio-frequency (RF) devices in the Ka band using moderate external fields, electrical or magnetic. This STTR program is targeted at developing ferroelectric and ferromagnetic tunable filters with the following specifications:

(i) low insertion loss, targeting < 1 dB,
(ii) high out-of-band rejection, targeting > 20 dB,
(iii) small size with preferably integrated solutions,
(iv) the ability to operate at high power levels, targeting > 2 Watts,
(v) low power consumption in the device and control circuit,
(vi) fast switching speed, and
(vii) temperature stability.

The Phase II project is divided into eleven tasks as shown in **Table 1**.

Table 1. Proposed Phase II Performance Schedule.

Phase II Task	Facility	Quarters							
		1	2	3	4	5	6	7	8
1. IMPROVE BST	nGimat								
2. BST TEMPERATURE STABILITY	nGimat								
3. IMPROVE FILTER DESIGN	nGimat/GT								
4. DEPOSIT BZN	nGimat								
5. FABRICATION/TESTING	nGimat/GT								
6. OPTIMIZE FERRITE FILMS	nGimat								
7. FERRITE FILTERS	nGimat/GT								
8. PROTOTYPING	nGimat/GT								
9. SCALE-UP	nGimat/GT								
10. CUSTOMER RELATIONS	nGimat								
11. REPORT	nGimat								

In this final reporting period, the device fabrication equipment was operational and there was no problem of metal peeling off during evaporation. The following outlines the progress in thin film deposition and device fabrication:

(1) In this reporting period, we optimized the Ba, Sr, and Ti ratio to get high tuning low insertion loss BST thin film for RF device fabrication. This was required due to a change in precursor lots with a different metal content. Thick metal using CPW pattern was put onto the BST samples. Tuning and insertion loss were measured so that the dielectric constant and figure of merit could be calculated. We selected of the best Ba, Sr and Ti ratio as a new standard value for BST deposition.
(2) We fabricated four of Georgia Tech designed 2-pole CPW Ka-band filters and nGimat designed Ring Ka-band filters. S-parameters for these samples are reported.
(3) We used dual-layer BST structure with different compositions to achieve a significantly more temperature stable BST thin film. The variation of capacitance vs temperature for one sample shows only 2 % range under a bias of 16 V in the temperature range of –40 to 120 ^{o}C. We will use this composition for future temperature stable BST thin film deposition.
(4) Since BZN sample has low insertion loss, wide temperature stable window, and decent RF tuning, it is an indispensible material for this Army project with a very low loss desired (<1dB). In the previous quarterly report, we reported that we deposited

several BZN samples with around 50 % tuning and 2 dB insertion loss at 67 GHz, and below 1dB over many GHz. We tried to repeat depositing BZN for Ka-band tunable filter fabrication. However, it seems that the deposition condition for tunable BZN deposition is very picky. There may be too many factors effecting the tunability of BZN: deposition composition, electrode processing, doping and BZN composition. Although sometimes we got some tunable BZN samples in this reporting period, we still have not achieved repeatable tunable BZN structures.

(5) We are still working on the device fabrication of Ka-band Substrate-Integrated Folded-Waveguide (SIFW) Filter designed by Ga Tech. We will submit the results to the TPOC and others in the future once we finish the fabrication and measurements.

2. Results and Discussions

2.1 BST composition optimization and electrical properties

In one of our on-going Air Force SBIR Phase II (contract # FA9451-10-C-0012) program, we developed BST thin films to get low insertion loss, high breakdown voltage, ferroelectric materials. In this Army effort we also used these films results to further study the BST electrical properties and to optimize the BST composition. Each time we get a different lot of precursor(s) the elemental weight % can change, thus throwing off the BST ratio. In this case we did get a precursor with undefined percentage change, so we had to refine the ratio of each precursor to achieve the best results.

Total nine samples are listed in **Table 2**. For comparison, the tuning, insertion loss and figure of merit (FOM) of different samples with various Ba, Sr, and Ti ratio are listed. The tuning is from E-shape capacitors of the CPW mask. The metallization is done at nGimat this time. Except the Ba, Sr and Ti composition ratio, other deposition parameters were kept constant. 1x1 cm *c*-plane sapphire was used as the substrate.

After considering the tuning, insertion loss, and FOM as well as the XRD results, we selected Ba/Sr ratio being 0.625 and (Ba+Sr)/Ti ratio being 0.75 as a standard ratio for final depositions in this report. The Georgia Tech designed 2-pole CPW Ka-band filter and nGimat designed Ring Ka-band filters are fabricated using BST diced from a coated 2" inch wafer. We deposited two 2 inch BST film samples, UR30D and UR30E. The UR30D's BST film thickness is around 230 nm, while UR30E's BST film thickness is around 200 nm. Total four tunable Ka-band filters were made, and their electrical properties with S-parameters are shown in the following section.

Figure 1 shows that area XRD detector pattern of some of BST samples. There is an XRD arc as indicated by the arrows appearing in the XRD pattern of 10167-03, 10177-02, 10196-01, while it disappears in the XRD pattern of UR30B and UR30C. The existence of XRD arc means that the some of the BST grain of BST film is randomly oriented (not single crystal). As we mentioned, UR30B and UR30D are our new standard BST. Without XRD arc in the XRD pattern of UR30B and UR30D indicates that they have high crystal quality and BST ratio and epitaxy conditions have been optimized. **Figure 2** shows the SEM image of standard BST sample UR30B. **Figure 3** shows the insertion and return loss measurement result up to 67 GHz for some of the BST samples.

Table 2. Average Tuning, Insertion Loss at 40 GHz, and Figure of Merit for different BST with various Ba, Sr and Ti ratio.

Sample #	Ba/Sr	Ba+Sr/Ti	Average Tuning	Film thickness (nm)	Insertion loss at 40 GHz (dB)	Figure of Merit (FOM)
10167-03	0.605	0.8	39.2	230	5.7867	6.7407
10168-01	0.675	0.9	43.4	230	6.4273	6.5656
10177-01	4.0	0.9	32.5	230	8.5506	3.9234
10177-02 (double layer)	4.0	0.9	31.5	330	7.7018	4.0606
	0.6	0.9				
10196-01	0.605	0.8	26.2	200	4.0132	6.4845
10196-02	0.675	0.9	28.9	180	5.0844	5.3582
10196-03	0.625	0.75	40.1	200	4.8531	7.937
UR30B (2 inch single layer) New standard	0.625	0.75		210		
UR30C-1 (2 inch double layer)	4.0	0.9	32.9	230	7.749	4.4053
	0.6	0.9				

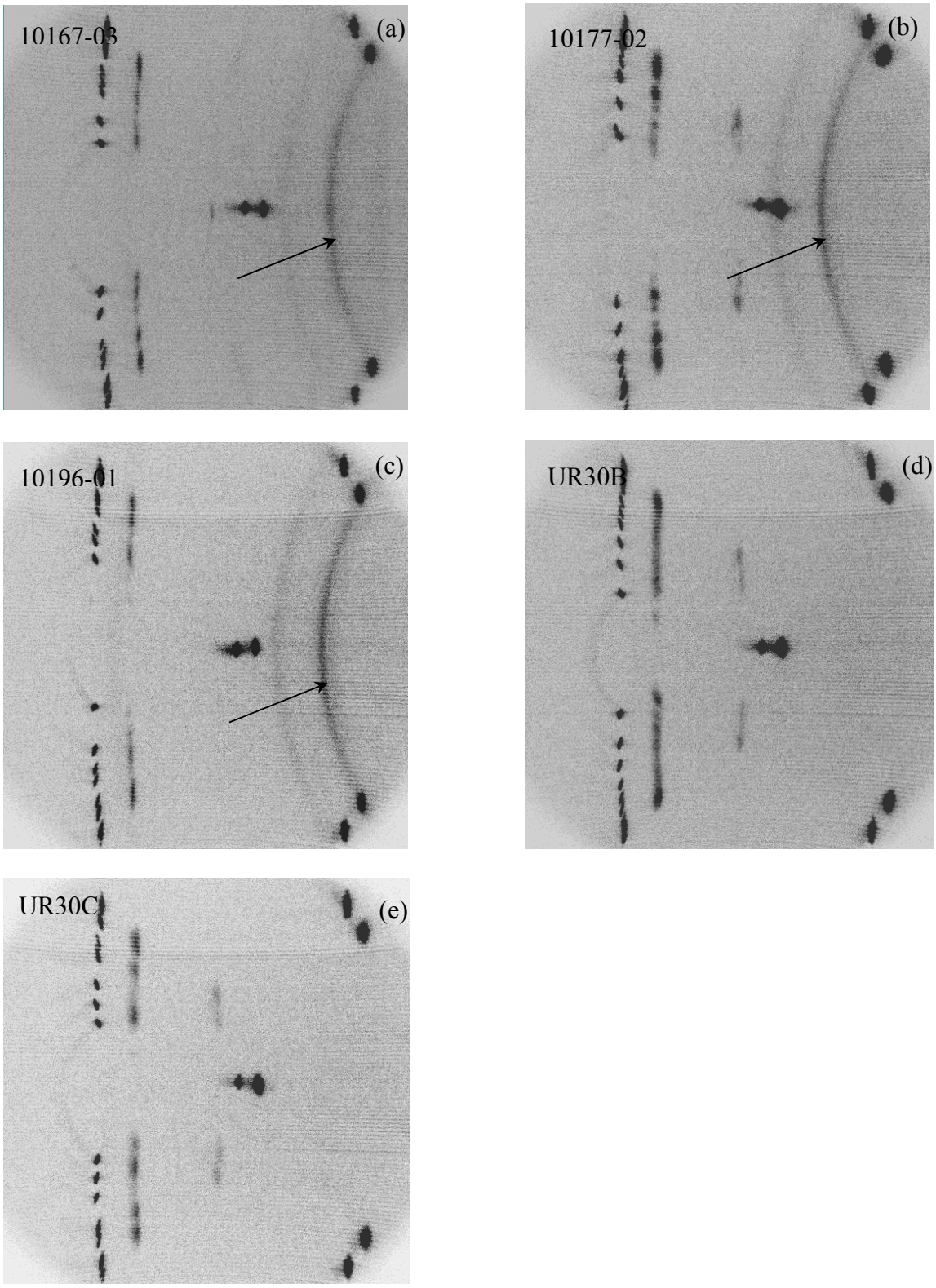

Figure 1. Area XRD detector pattern of some of BST samples. (a) 10167-03; (b) 10177-02; (c) 10196-01; (d) UR30B; and (e) UR30C. The lack of arc in UR30B and UR30C indicates their higher quality.

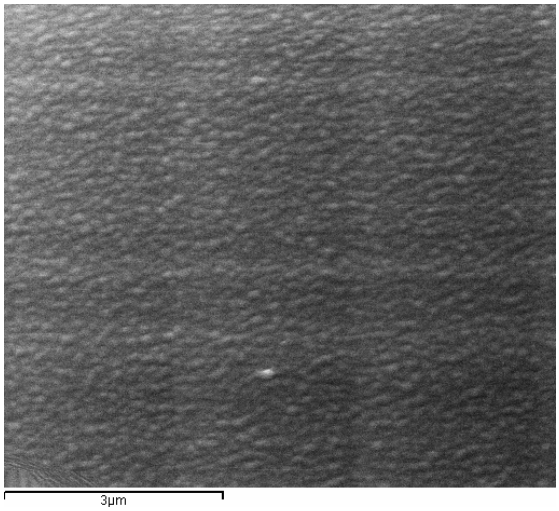

Figure 2. SEM micrograph of standard BST UR30B on *C*-plane sapphire.

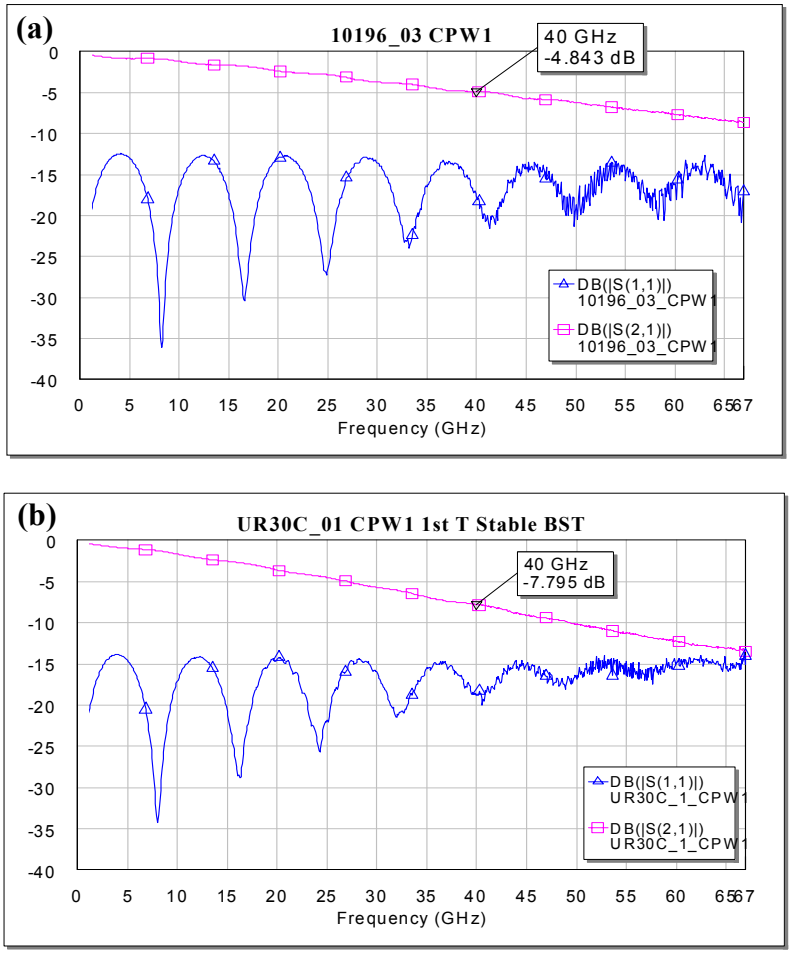

Figure 3. Insertion and return loss measurement results for BST composition study samples. (a) RF10196-03 with composition of Ba/Sr ratio 0.625 and (Ba+Sr)/Ti ratio 0.75 (We select this composition as our new standard single layer BST); and (b) UR30C with composition of : (a) bottom layer Ba/Sr ratio 4.0 and (Ba+Sr)/Ti ratio 0.9 and (b) top layer Ba/Sr ratio 0.6 and (Ba+Sr)/Ti ratio 0.9.

2.2. BST temperature stable film deposition and electrical measurements

DoD has a wide temperature range for various application. To have enhanced temperature stable BST capacitors, two-layer BST structure was used with different BST composition and temperature response. Because the dual BST layers have different Curie temperature due to their different composition, their temperature response will compensate with each other, which results in enhanced stable temperature response in a wide temperature range (from – 40 to 120 ^{o}C).

Two samples with different composition of dual layer were deposited: (a) UR30C and (b) RF10219-01. For UR30C, the composition of bottom layer is: Ba/Sr being 4.0 and (Ba+Sr)/Ti being 0.9; the composition of top layer is: Ba/Sr being 0.6 and (Ba+Sr)/Ti being 0.9. For RF10219-01, the composition of bottom layer is: Ba/Sr being 3.5 and (Ba+Sr)/Ti being 0.75; the composition of top layer is: Ba/Sr being 0.5 and (Ba+Sr)/Ti being 0.75.

The measured temperature response of BST temperature stable capacitors from UR30C and RF10219-01 are shown in **Figure 4**. **Table 3** shows the variation of capacitance vs Temperature for samples RF10219-01. From Figure 4, sample RF10219-01 has better temperature response than UR30C: less capacitance variation and higher Q-factor. The capacitance variation of sample RF10219-01 in the temperature range of –40^{o} and +120 ^{o}C is about 5 % when the applied voltage is at 0V and only **2 %** at 16 V, respectively. The tuning of sample RF10219-01 is around 44 % in the entire temperature range.

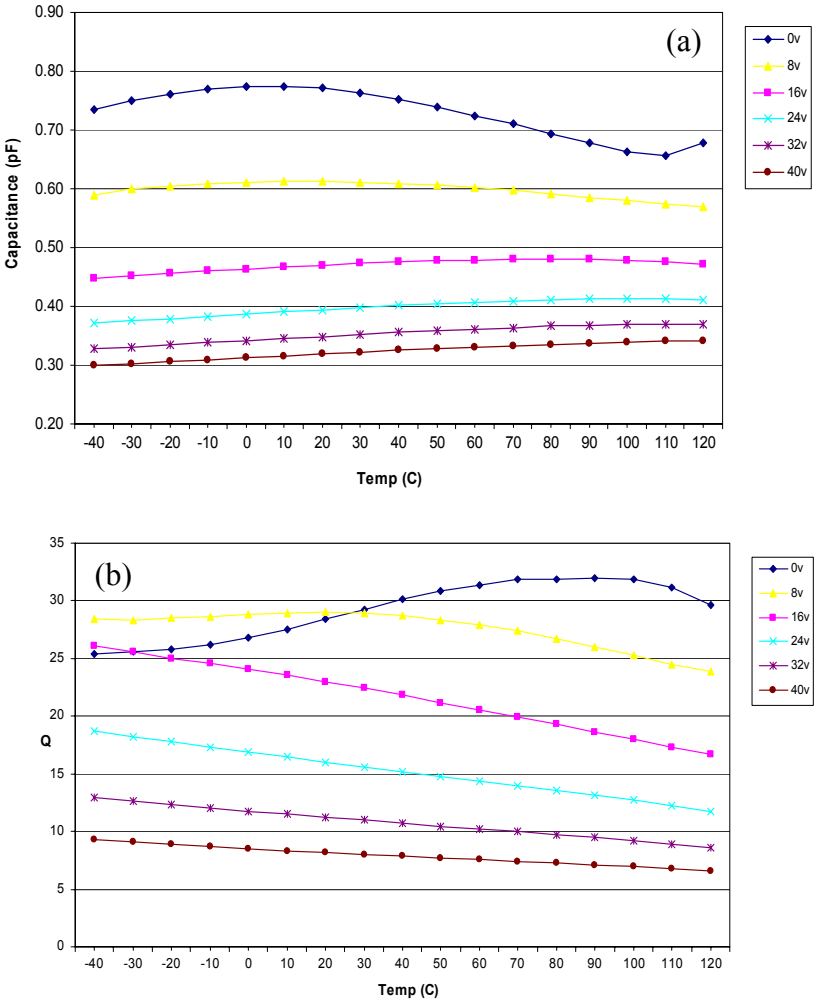

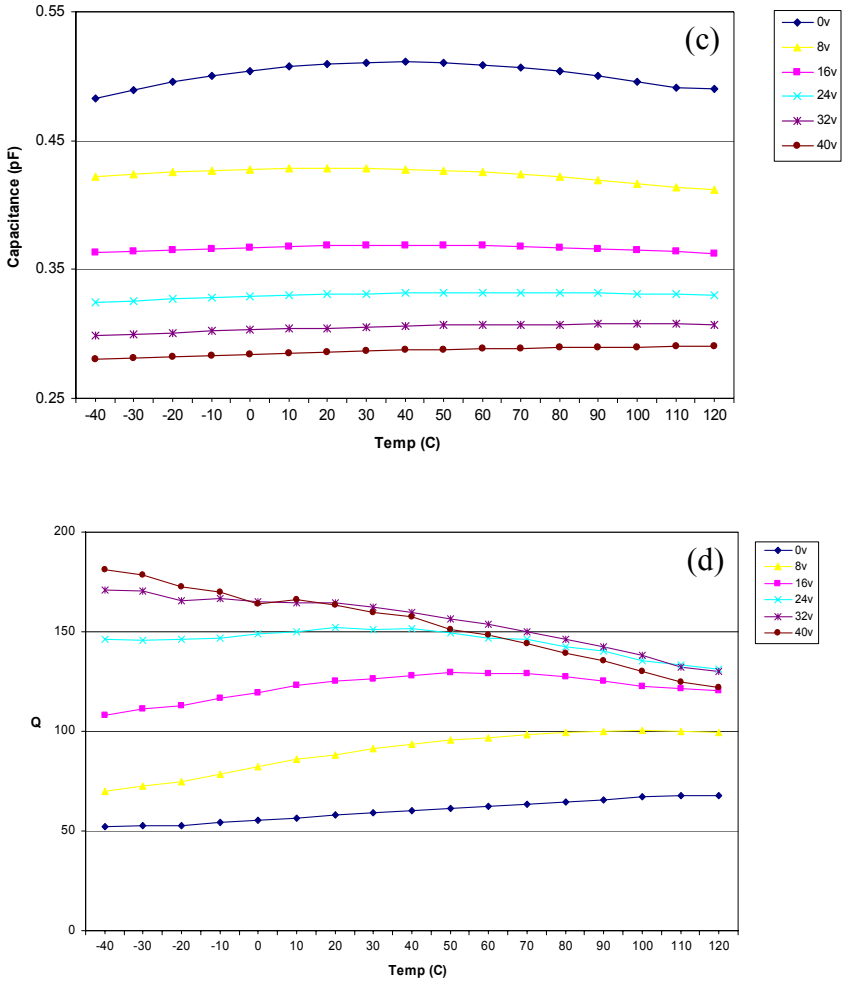

Figure 4. Temperature response of two dual-layer BST samples. Sample UR30C (a) Capacitance vs Temperature; (b) Q-factor vs Temperature, and sample UR10219-01 (c) Capacitance vs Temperature; (d) Q-factor vs Temperature.

Table 3. The variation of capacitance vs. Temperature for sample RF10219-01.

Temp	0v	8v	16v	24v	32v	40v	Tuning
-40	0.483	0.422	0.363	0.325	0.299	0.280	42%
-20	0.495	0.426	0.365	0.327	0.301	0.282	43%
0	0.504	0.428	0.367	0.329	0.303	0.284	44%
20	0.510	0.429	0.368	0.331	0.305	0.286	44%
40	0.511	0.428	0.369	0.332	0.306	0.287	44%
60	0.509	0.426	0.368	0.332	0.307	0.289	43%
80	0.504	0.422	0.367	0.332	0.308	0.290	43%
100	0.495	0.416	0.365	0.331	0.308	0.290	41%
120	0.490	0.412	0.363	0.330	0.307	0.290	41%
Temp Variation	5%	4%	2%	2%	3%	4%	

From the temperature study measurement results, we selected 3.5/0.75 and 0.5/0.75 dual layer as the standard temperature stable BST ratio for this projects future device fabrication. We have a commercial application for which we are hoping to make many phase shifters with this composition.

2.3. BZN film composition optimization and electrical measurements

We reported that the BZN-based capacitors has a tuning of 35 % with BZN composition of 1.13:1:0.88 on *c*-plane sapphire substrate in the previous quarterly report. In this reporting period, we deposited six more BZN samples with different composition ratios, deposition temperature and film thickness, and tried to repeat the previous results. We found that two of the samples have similar tuning as before. When we tried to redo the deposition using the same deposition conditions, the BZN film did not tune again. From our experience, the tuning of final sample is very sensitive to the BZN deposition condition including composition, temperature, doping, cooling down rate (different cooling rate will result in different phase of BZN material), and possibly electrode processing. To get a repeatable and tunable BZN thin film, we still need to do more extensive research.

Figure 5 shows the area XRD detector pattern of five BZN thin films. The electrical properties of the six BZN samples are listed in **Table 4**, previous tunable BZN sample (09337-02) is also listed as a reference.

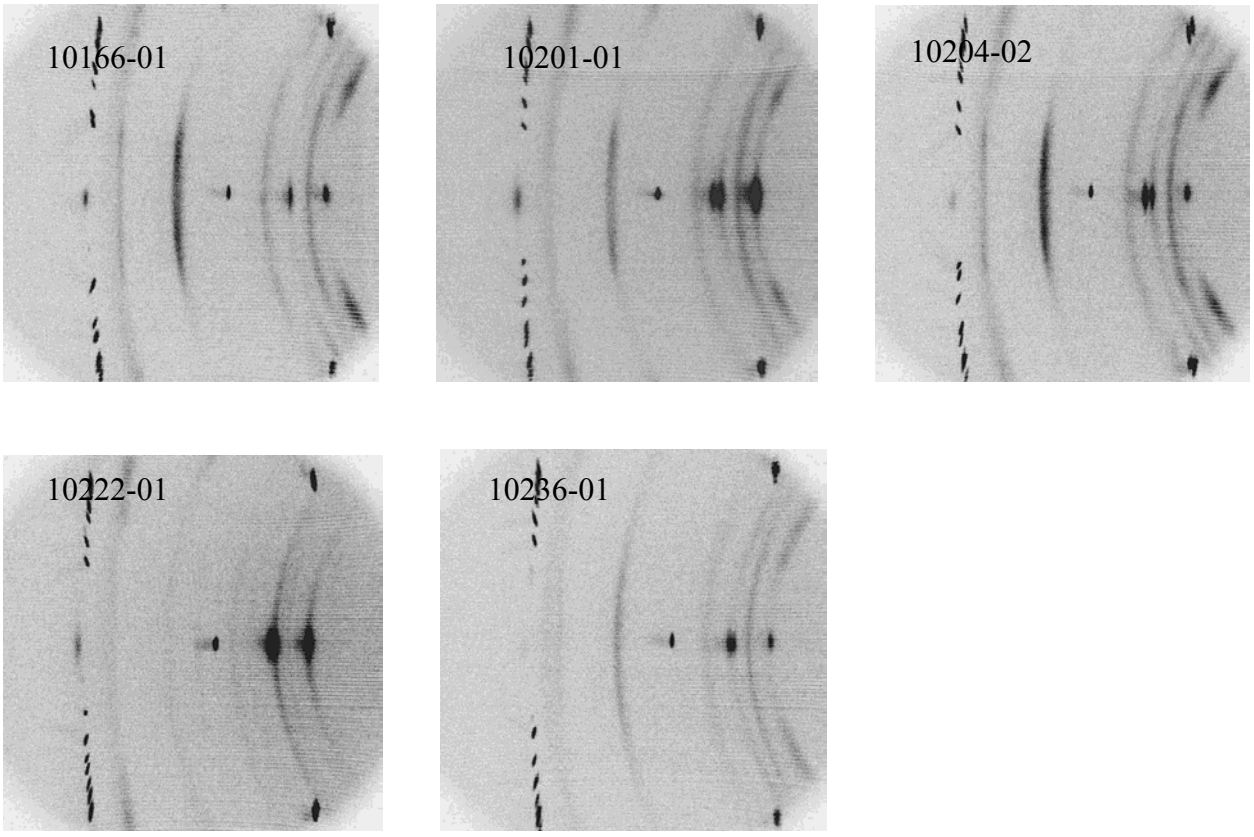

Figure 5. Area XRD detector pattern of BZN samples. (a) 10166-01; (b) 10201-01; (c) 10204-02; (d) 10222-01; and (e) 10236-01. Their compositions are listed in **Table 4**.

Table 4. List of deposited BZN samples with deposition conditions and electrical measurement results (@ 1MHz).

Sample ID	Solution Ratio (Bi:Zn:Nb)	Deposition Temp (°C)	Thickness (nm)	Dopant	Tuning of test capacitor at 20 V	Tuning of different capacitor in CPW structure at 40 V(%)	
						C1	CPW #2 (5/10)
09337-02 (09323-01) (REF)	1.13:1.0:0.88	835	300	Unintentional	43 %	4.0 %	1.4 %
10166-01	1.06:1:1.08	835	300	1% Fe	4.6 %		
10201-01	1.06:1:1.08	800	300	1% Fe		5.5 %	3.0 %
10204-02	1.13:1.0:0.88	800	300	No		3. 4 %	1.48 %
10216-01	1.06:1:1.08	800	230	1% Fe	N/A	N/A	N/A
10222-01	1.06:1:1.08	800	230	No	5.8 %		
10236-01	1.06:1:1.08	800	230	1% Fe	4.3 %		

To measure electrical properties of insertion loss at both low and high frequencies, coplanar waveguide (CPW) were fabricated on selected samples by a lift-off process at *n*Gimat. Capacitance and dielectric loss at low frequencies are measured by HP 4285A Precision LCR meter. Microwave properties at high frequencies are measured by a network analyzer at Georgia Tech.

Figure 6 shows the schematics of the typical 7 mm long CPW structures with (a) 70 μm gaps and a 30 μm center conductor (signal), and (b) 10 μm gaps and a 5 μm center conductor. These CPW structures are referred as CPW1 and CPW2 structures, respectively. Return and insertion losses were measured on these CPW structures at different frequencies up to 65 GHz.

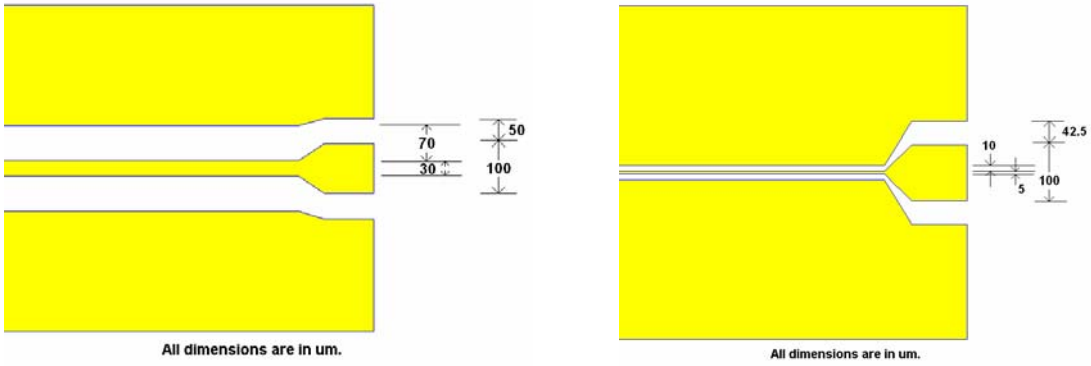

(a) CPW1 structure (b) CPW2 structure

Figure 6. Schematics of the 7mm long CPW structures (a) with 70 μm gaps and a 30 μm center conductor (signal) (CPW1) and (b) with 10 μm gaps and a 50 μm center conductor (signal) (CPW2).

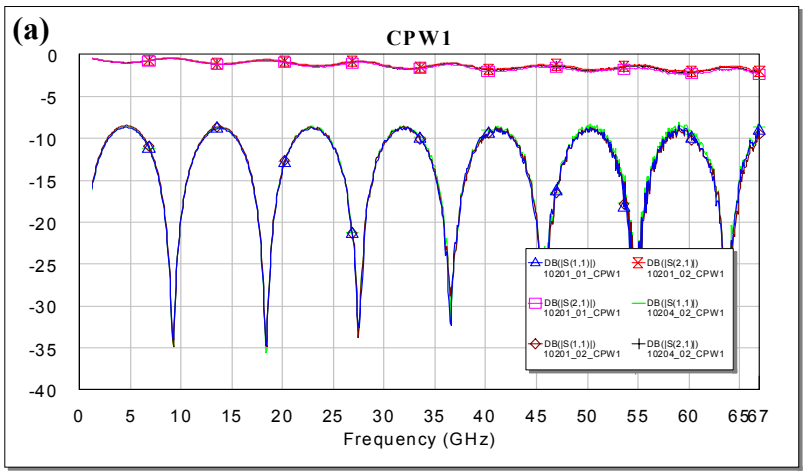
(a)
CPW1
0
-5
-10
-15
-20
-25
-30
-35
-40
0 5 10 15 20 25 30 35 40 45 50 55 60 6567
Frequency (GHz)
DB(|S(1,1)|) 10201_01_CPW1
DB(|S(2,1)|) 10201_02_CPW1
DB(|S(2,1)|) 10201_01_CPW1
DB(|S(1,1)|) 10204_02_CPW1
DB(|S(1,1)|) 10201_02_CPW1
DB(|S(2,1)|) 10204_02_CPW1

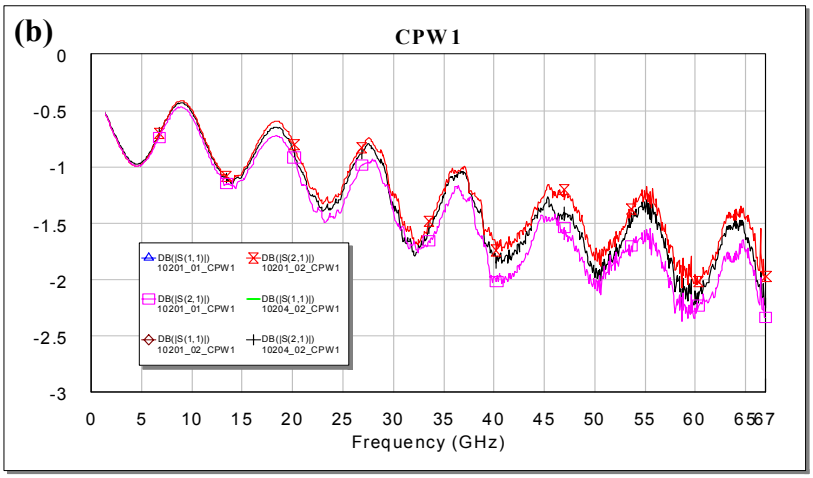
(b)
CPW1
0
-0.5
-1
-1.5
-2
-2.5
-3
0 5 10 15 20 25 30 35 40 45 50 55 60 6567
Frequency (GHz)
DB(|S(1,1)|) 10201_01_CPW1
DB(|S(2,1)|) 10201_02_CPW1
DB(|S(2,1)|) 10201_01_CPW1
DB(|S(1,1)|) 10204_02_CPW1
DB(|S(1,1)|) 10201_02_CPW1
DB(|S(2,1)|) 10204_02_CPW1

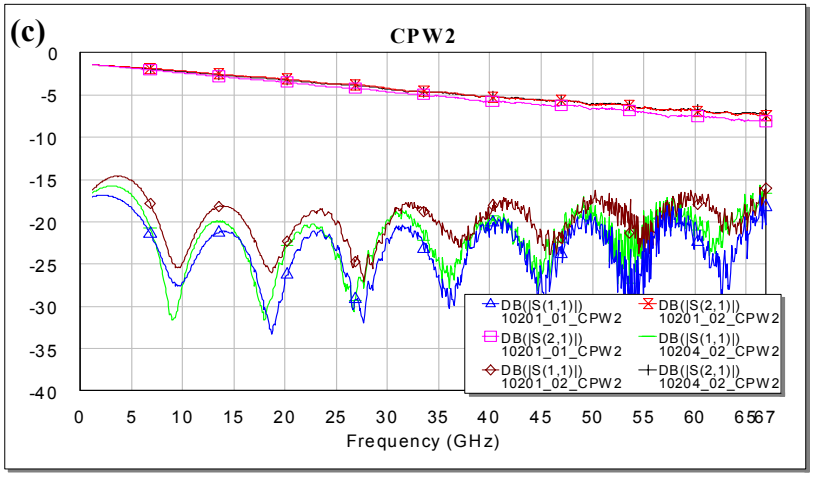
(c)
CPW2
0
-5
-10
-15
-20
-25
-30
-35
-40
0 5 10 15 20 25 30 35 40 45 50 55 60 6567
Frequency (GHz)
DB(|S(1,1)|) 10201_01_CPW2
DB(|S(2,1)|) 10201_02_CPW2
DB(|S(2,1)|) 10201_01_CPW2
DB(|S(1,1)|) 10204_02_CPW2
DB(|S(1,1)|) 10201_02_CPW2
DB(|S(2,1)|) 10204_02_CPW2

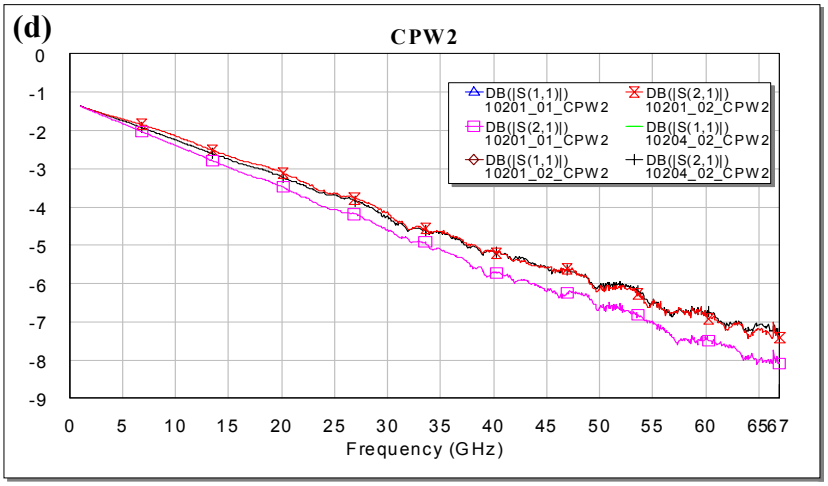

Figure 7. Insertion and return loss measurement results for BZN samples: RF10201-01, RF10201-02, and RF10204-02. (a) return and insertion loss on CPW1 structure, (b) zoomed insertion loss on CPW1 structure, (c) return and insertion loss on CPW2 structure, and (d) zoomed insertion loss on CPW2 structure.

Figure 7 shows the measured return and insertion loss of three BZN samples: RF10201-01, RF10201-02, and RF10204-02. The insertion loss of these samples are as low as around 2 dB from 0 to 67 GHz no matter what the compositions and deposition conditions are. If we can reduce the 0.5 dB insertion loss from the thick metal layer by increasing the thick metal layer thickness and improve the metal/BST interface states, BZN could be an indispensible material for low insertion loss RF device application. The consistency of tunability must be addressed.

2.4. Ka-band tunable Filter Devices

Figure 8 shows the picture of 2-pole CPW Ka-band tunable filter designed by Georgia Tech. (also shown in Figure 15 of the report #2). **Figure 9** shows the picture of nGimat designed Ka-band tunable ring filter (also shown in Figure 17(b) of the report #2). As we mentioned before, we deposited two 2" BST wafer using our new standard BST composition and deposition conditions. Total four samples were fabricated using nGimat and Ga Tech designed Ka-band tunable filter structures.

Figure 10 shows the measured S-parameters of 2-pole Ka-band filter under bias voltage from 0V to 30 V. (a) UR30D-05, (b) UR30E-01. From our experience, low capacitance will result in low tuning. The tuning for both of these samples are low maybe because in this design the capacitance is small (around 0.06 pF) and has large percentage of fringe field capacitance (not in BST) that does not tune.

Figure 11 shows the measured S-parameters of the most recently made Ka-band Ring filter using the current standard BST films. We did not deposit the ground metal on the back of the sapphire substrate and used the chuck on the probe station as its ground. Directly deposited metal does affect the devices performance. This filter was measured without bias (or at 0V only). We have previously made the same filter with ground metal deposited on the back of the substrate and the tuning of this filter from 0 to 30 V was demonstrated in Figure 16 of the report #2. (or Figure 12 of this report). We expect that there are several μm air gap between the bottom of the sapphire substrate and the ground chuck. This air gap should have a minimal degradation on the insertion and return loss measurements. The insertion loss for the samples UR30D-04 and UR30E-01 are about 2.8 dB at around 32 GHz, while the return loss for both of these samples are less than 15 dB The sample UR30E-02 has return loss larger than 15 dB around 35 GHz and the insertion loss of about 4 dB at around 33 GHz. Note that the filter on UR30E-02 has both the upper and lower cutoff at higher frequencies than the ones on UR30D-04 and UR30E-01. We suspect

that this filter has a wider gap between the electrodes in the capacitor area, resulting in smaller capacitance.

The three filters above have been fabricated using nGimat's new standard BST films. An identical filter on UR18C-06 (thickness in the range of 200 to 230 nm) has been made using one of the previous BST films, and its measured responses are presented in Figure 16 of the report #2. For readers' convenience, the old filter's responses are repeated in Figure 12 here with 0V and 30V insertion loss marked at the center of the passband. The filter using the new standard BST film has a slightly higher insertion loss of 2.75 dB compared to 2.3 dB of the filter using old BST film. The slight difference in insertion loss may be due to a number of reasons including BST film thickness, BST and metal contact interface, or the small air gap between the substrate and the ground in the three recently made filters etc.

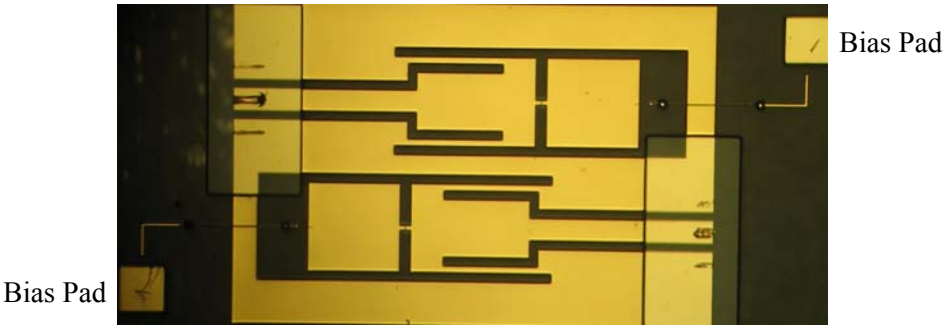

Figure 8. Photo of Georgia Tech designed 2-pole Ka-band tunable filters biased through RF electrodes.

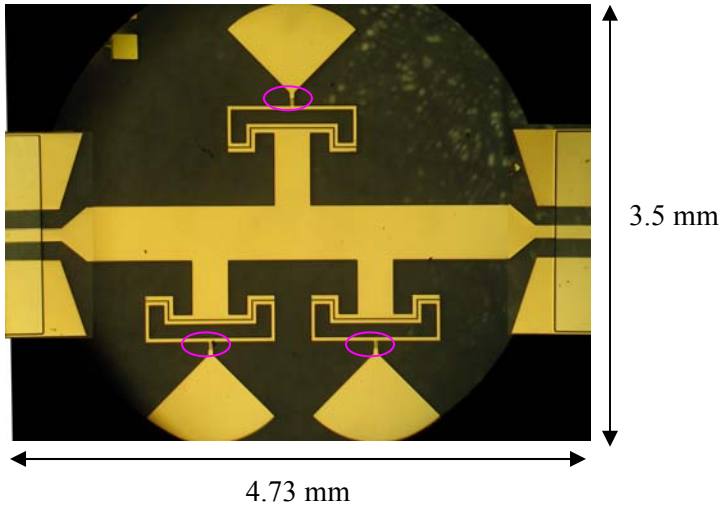

Figure 9. Picture of a fabricated nGimat designed Ka-band tunable Ring filter.

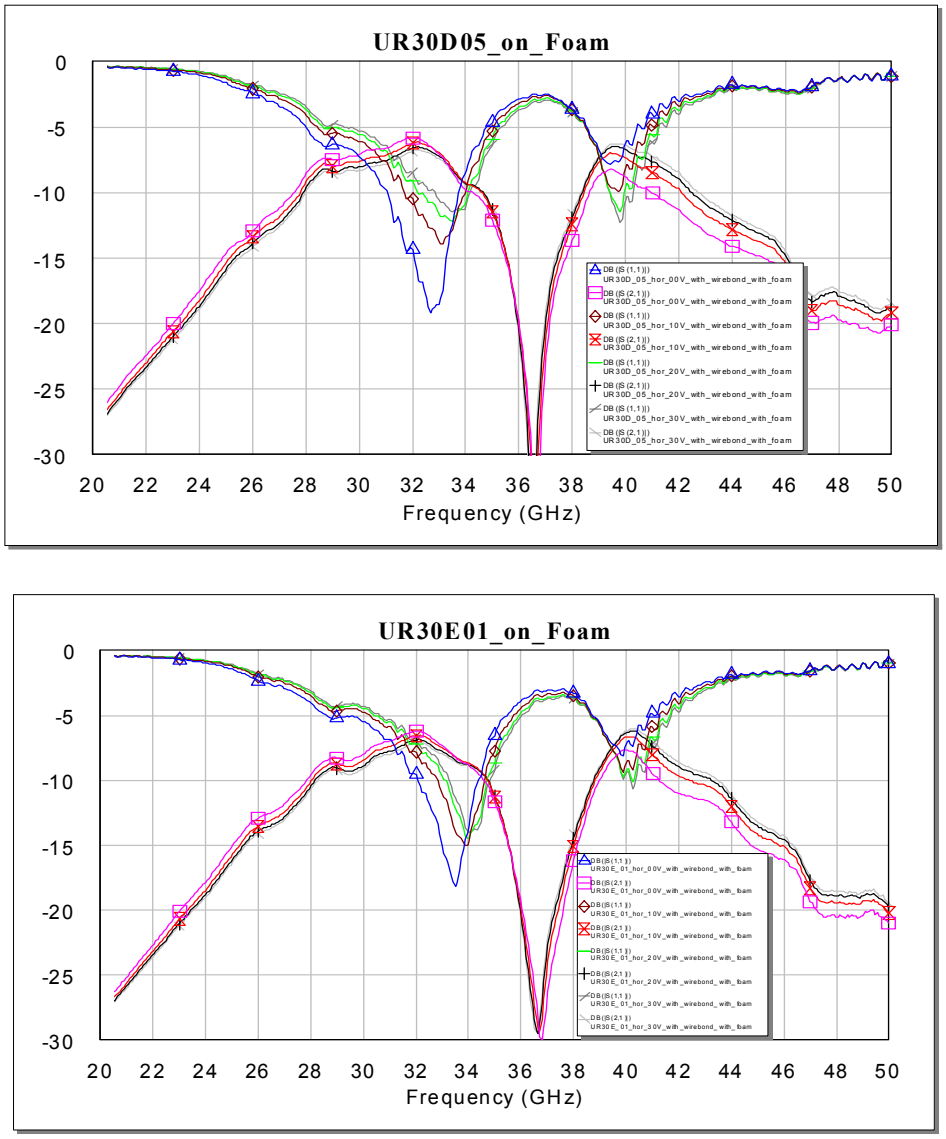

Figure 10. Measured S-parameters of 2-pole Ka-band filter under bias voltage from 0V to 30 V. (a) UR30D-05, (b) UR30E-01. From our experience, low capacitance will result in low tuning. The tuning for both of these samples are low maybe because in this design the capacitance is small (around 0.06 pF).

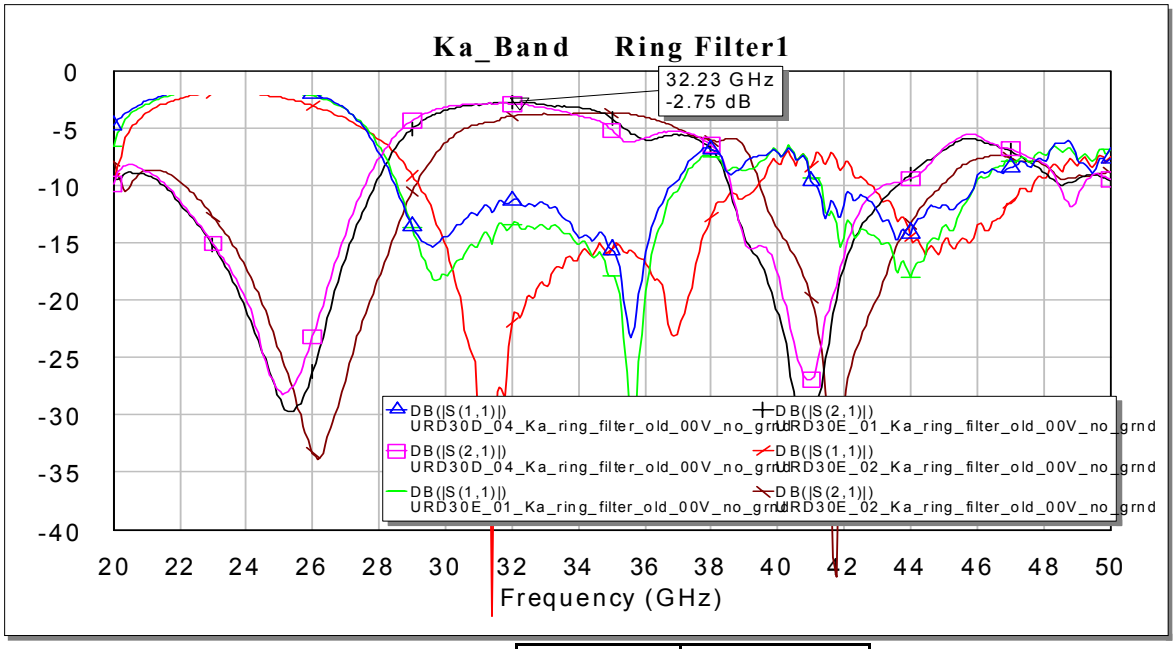

	Return loss	Insertion loss
UR30D-04	Blue	Pink
UR30E-01	Green	Black
UR30E-02	Red	Brown

Figure 11. Measured S-parameters of Ka-band Ring filter without bias

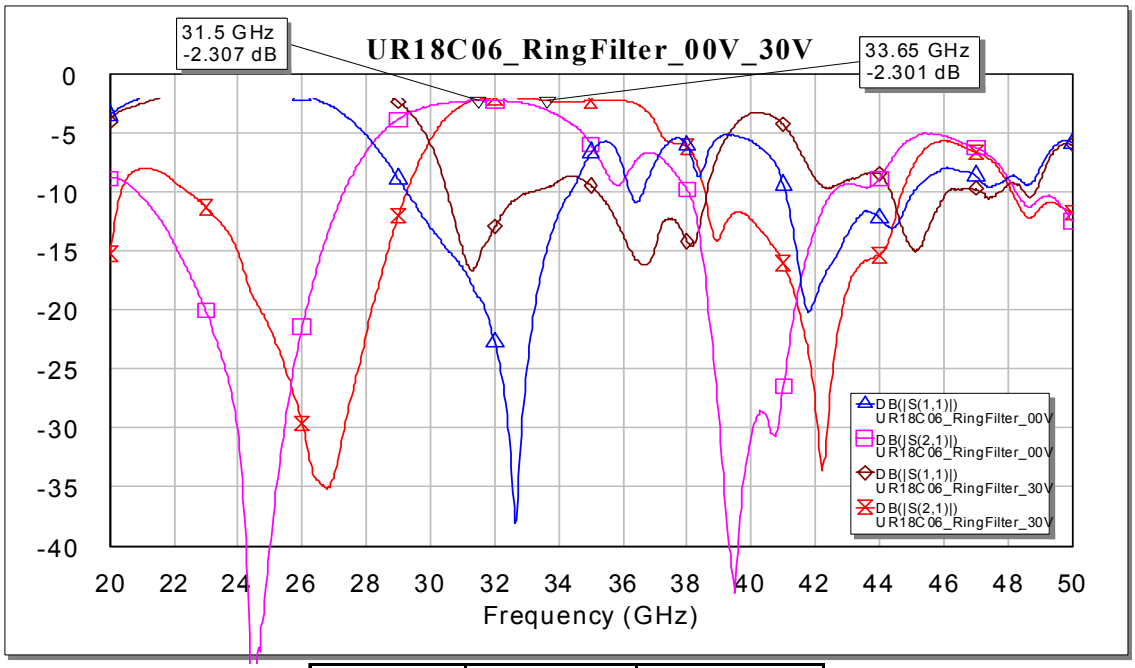

Bias (Volt)	Return loss	Insertion loss
0	Blue	Pink
30	Brown	Red

Figure 12. The responses of the filter in Figure 10 fabricated for the report #2 using previous BST film, but this one has bottom metallization.

3. STTR Partner final report from Ga Tech

1

Development of Tunable Ka-band Filters

Final Report

Ben Lacroix, Stanis Courreges, Yuan Li, Carlos Donado and John Papapolymerou

School of Electrical and Computer Engineering
Georgia Institute of Technology
Atlanta, GA 30332

Introduction/Summary

Georgia Tech has designed several filters operating in Ka-band. These filters are built on Sapphire and use integrated BST thin films as tuning elements. The fabrication is conducted by nGimat, Inc. Four different approaches are presented in this report.

The first filter is a 3-pole filter based on a CPW (Coplanar Waveguide) topology and includes 6 BST capacitors. It is built on a Sapphire substrate and tunes from 29 to 34 GHz (17%). The fractional bandwidth is about 10-12%. Insertion loss of only 2.5 dB is measured when the BST capacitors are biased with 30 V.

The second CPW filter consists of two resonators whose physical/electrical lengths can be changed by coupling each resonator with an additional piece of line which acts like a loading capacitor. Therefore, the center frequency can be tuned. The measured tuning appears to be lower than expected. Several issues are discussed.

The third filter is also based on a CPW topology, and uses 4 BST capacitors located at the end of the resonators in order to make the filter tune. This design is based on cross-coupled resonators. A trade-off between performance and tuning is discussed.

Finally, the fourth part demonstrates the design and implementation of a two-pole, Tunable Folded Waveguide Filter (TFWF) on sapphire and with tuning provided by barium strontium titanate (BST) capacitors. The filter operates in the Ka-band and has a simulated tuning range of 10% (27.72 GHz to 30.50 GHz).

Part I

3-pole tunable Ka-band filter

I. 1/ Filter design:

The design objective is a three-pole tunable BPF using BST capacitors for Ka-band with a center frequency f_0 in the Ka-band (26–40 GHz), a fractional bandwidth of around 10-12%, a return loss of 20 dB, a frequency tuning greater than 15% and a minimum OIP3 value of 15 dBm. Figure I.1 shows the three-pole coplanar tunable filter loaded with six BST capacitors (3 on each side).

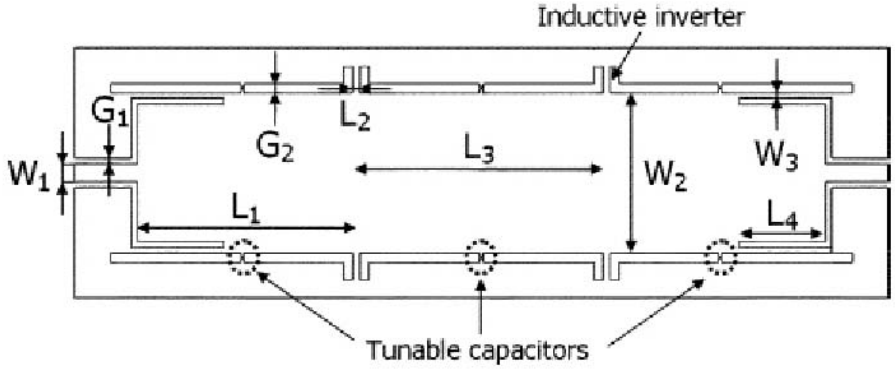

Fig. I.1. Layout of the designed three-pole tunable bandpass filter using 6 BST capacitors.

A coplanar waveguide configuration is chosen to reach the specifications of the frequency tuning and the integration of the circuit. The filter is designed by cascading three half-wavelength resonators with inductive impedance inverters. Since the electric field is maximal at the middle of the resonators, a maximum frequency shift can be achieved by loading tunable capacitors at this position. The filter is fed by original feedlines: the first part is a 50 Ω line connected to a wider short circuited line. With this feeding structure, the filter does not need bridges, and the external quality factor, Q_{ext}, can be optimized easily by modifying the length L_4, and the width W_3. It is also possible to get a wider resonator by keeping the same slot gap, which can increase the unloaded quality factor Q_0 of the filter.

The filter is made on a sapphire substrate (ε_r=10, tan δ < 0.0001 at 10 GHz). The metallization of the filter is a 2-µm thick copper. In order to meet the specifications, a coupling matrix is chosen with $R_{in} = R_{out} = 1.082$ and $k_{12} = k_{23} = 1.030$. The dimensions of the filter, the size of the feedlines and the width of the inverters are then adjusted in order to optimize the simulated S-parameters. A hybrid simulation is used to model the filter with the BST capacitors: the layout of the filter is simulated and includes internal ports at the capacitors locations. A RC lumped component model is used to represent the BST capacitor and its intrinsic loss. A capacitance ratio of 3:1 is considered (60 fF/20 fF) with a series resistance of 4 ohms. Then, the dimensions are optimized again with the loaded capacitors (Table I.1). The final size of the filter is 4560 µm x 1400 µm.

Table I.1 – Optimized dimensions of the designed 3-pole filter

Parameter	(µm)	Parameter	(µm)	Parameter	(µm)
W_1	100	L_1	1228	L_4	485
W_2	900	L_2	40	G_1	35
W_3	30	L_3	1407	G_2	50

The simulated response is shown in Figure I.2. The center frequency of the filter tunes from 28 GHz up to 34 GHz (21%) with a capacitance range of 60 to 20 fF. The fractional bandwidth ranges from 11% to 13.2% and the insertion loss, taking into account 4 series resistors, is between 3.8 dB (with C = 60 fF) and 2.8 dB (with C = 20 fF).

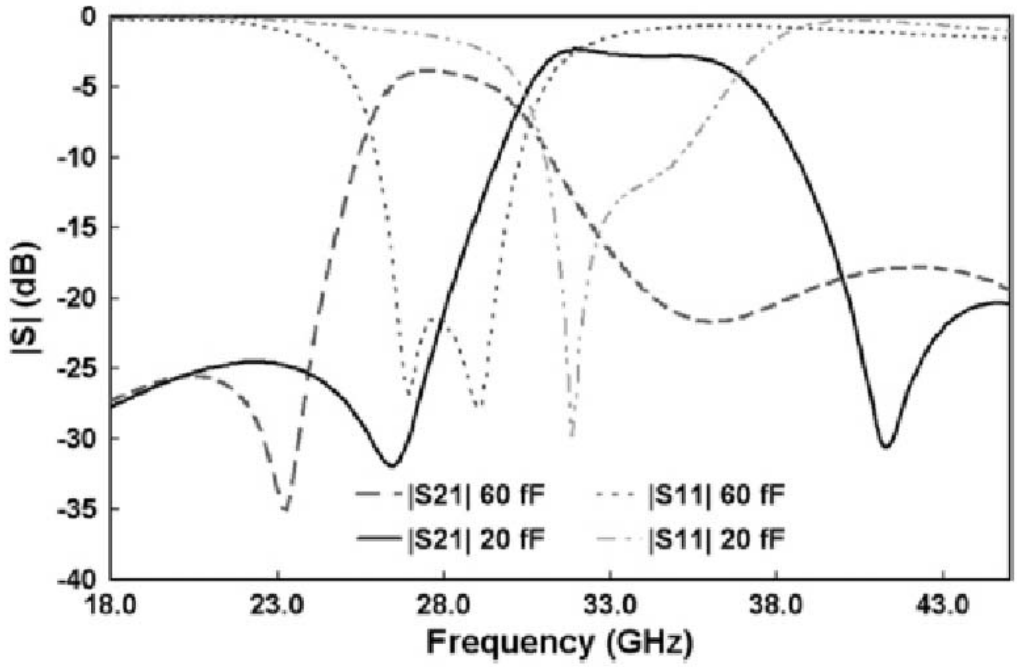

Figure I.2 – Simulated response of the designed 3-pole filter (C = 60 fF and C = 20 fF).

I. 2/ Fabrication:

The fabricated filter is presented in Figure I.3. A specific bias network has been designed to bias the BST capacitors. At 1 MHz, the capacitor values are ranging from 67 fF at 0 V to 27 fF at 30 V, resulting in a quality factor of 85 and 520 respectively.

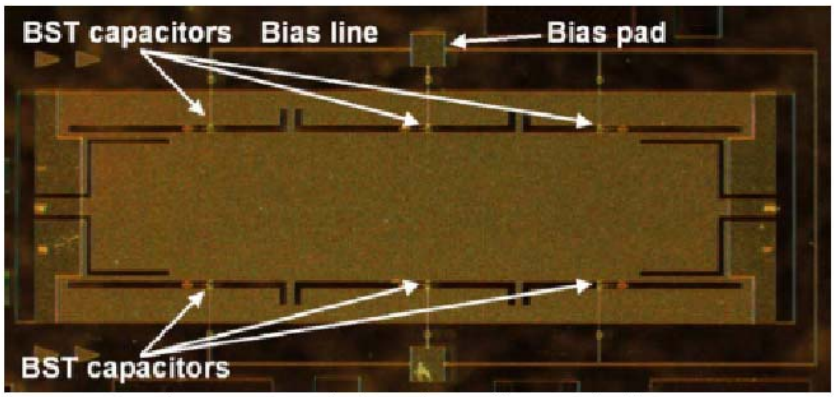

Figure I.3 – Fabricated tunable 3-pole filter.

I. 2/ Measurements:

A. S-parameters measurements

The measurements are performed using an Agilent Vector Network Analyzer 8510 C calibrated with the Short-Open-Load-Through (SOLT) standard. The bottom side of the coplanar filter (without ground plane) is fixed on foam, which has a permittivity close to 1, to imitate air. Then, the S-parameters are measured by using a probe station with bias voltages ranging from 0 V up to 30 V. Figure I.4 shows the measured return loss whereas Figure I.5 presents the measured insertion loss. The frequency tunes from 29 GHz, without bias voltage, up to 34 GHz with a voltage of 30 V. The frequency tuning is 17.2% and is close to the simulated value. The fractional bandwidth ranges from 9.5% up to 12.3%. For this technology, the filter has good insertion loss and return loss levels of 6.9-2.5 dB, and 24-13 dB, respectively, with a DC bias varying from 0 to 30 V at room temperature. This new filter, including the bias lines, has a better transmission coefficient outside the pass band at the highest frequencies: 25 dB instead of 15 dB.

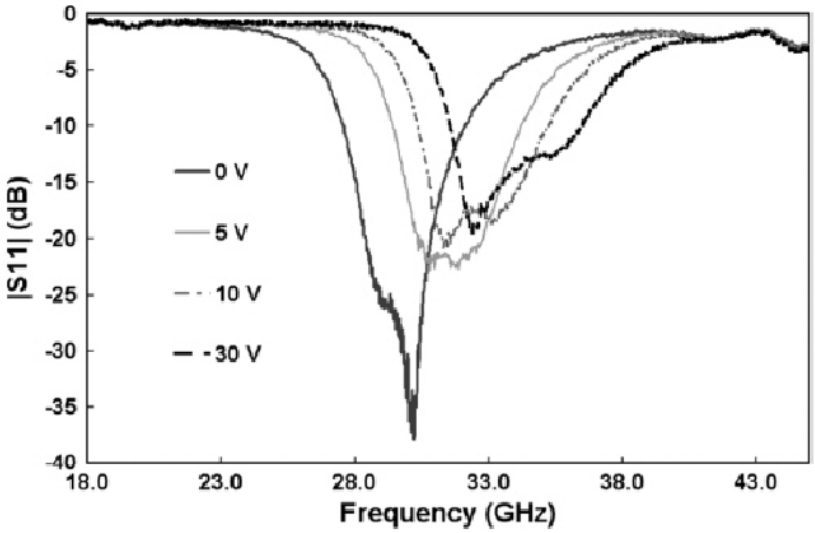

Figure I.4 – Measured return loss.

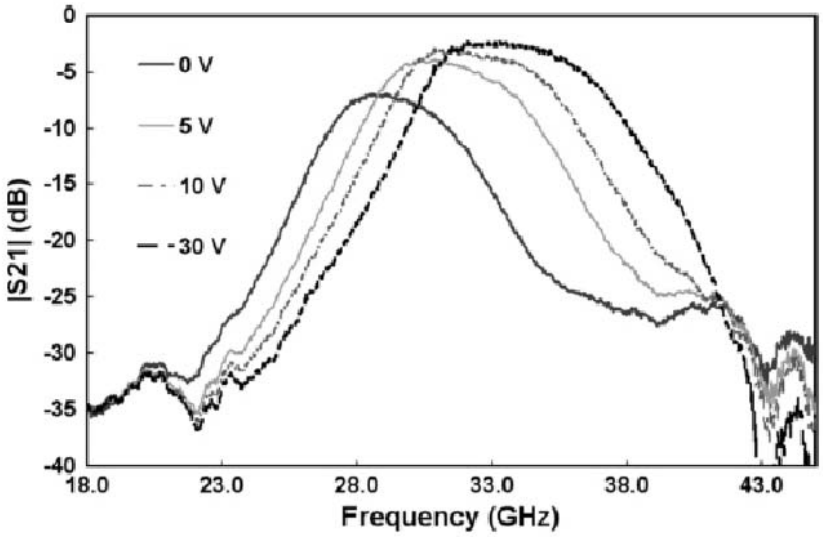

Figure I.5 – Measured insertion loss.

A. OIP3 measurements

The third order intercept point of the filter was measured on an integrated wafer-level RF measurement system capable of measuring noise, load pull, S-parameters, and intermodulation distortion up to 40 GHz without lifting the RF probes. To ensure accurate measurements, the system power level is calibrated with the reference plane located at the probe tips. This can be done by first measuring the insertion loss of the input and output RF blocks at the cable level. After an on-wafer thru-reflect-line (TRL) calibration, the insertion loss of the probes and tuners is calculated by successive one-port measurements using an open, short, and load standard at the output of each tuner. The probes are contacted to the wafer-level thru standard during these measurements. With the insertion loss known up to the probe tips, the power level can be accurately calculated using a power meter and simple addition and subtraction. Third order intercept was calculated by injecting two sinusoids at various frequency spacings. The power level of the primary tones and their third order intermodulation terms at (2f1-f2) and (2f2-f1) are then measured on a spectrum analyzer while the filter is still in the pass band of operation. The output third order intercept point can then be calculated using Eq. (1):

$$OIP_3(\mathrm{dBm}) = \frac{\Delta P(\mathrm{dB})}{2} + P_{out}(\mathrm{dBm}). \qquad (1)$$

Figure II.6 presents the OIP3 results with different bias voltages: 0 V, 10 V and 30 V. The OIP3 measurements are greater than 15 dBm with frequency spacings of 100 kHz, 300 kHz and 1 MHz. These results satisfy the specifications. Also, the filter uses tunable capacitors with simple shaped electrodes. The level of OIP3 could be improved by using other shapes of electrodes.

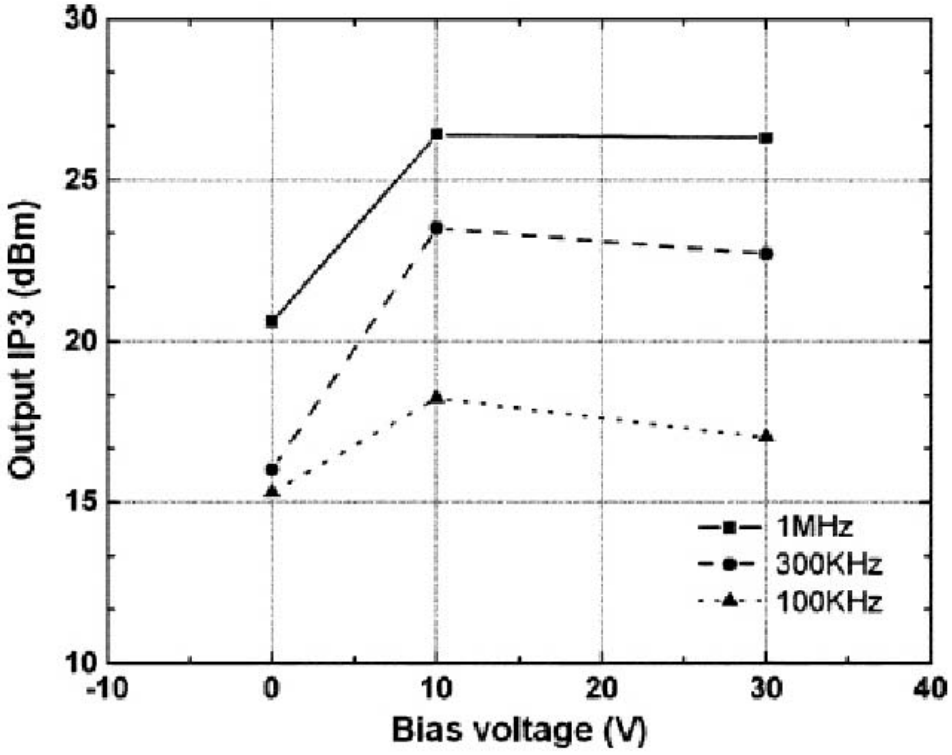

Figure II.6 – Output IP3 versus bias voltage for different frequency spacings.

Part II

2-pole tunable Ka-band filter

II. 1/ Filter design:

The designed filter is presented in Figure. II.1.

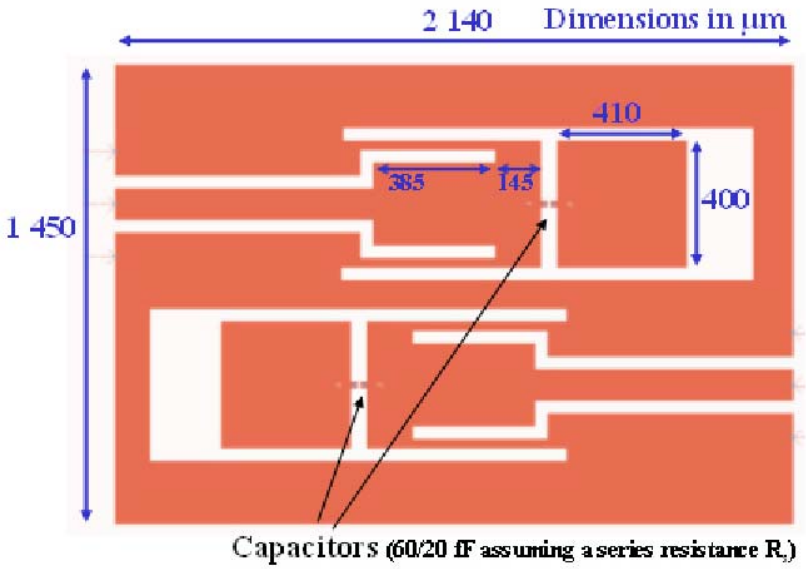

Fig. II.1. Layout of the designed two-pole tunable bandpass filter operating in Ka-band.

This filter consists of two resonators whose electrical lengths can be changed by tuning the BST capacitor. The rectangular pieces (410 um x 400 um) act like loading capacitors or an extension of the resonators. It could be seen as a change of the physical length if the BST capacitor was an ideal switch (in that case, there would be only two states). The feedlines are similar to the ones used for the 3-pole filter presented in Section I. The dimensions of the feedlines as well as that of the resonators and the additional parts are optimized in order to get good insertion loss and return loss levels. As in the previous Section, a lumped capacitor with a series resistance is used to model the BST capacitor: since the resistance value of the BST capacitor might be high at the operating frequency range, simulations with R = 4 ohms and R = 20 ohms have been performed in order to make sure that the insertion loss can still satisfy the specifications. The capacitor value tunes from 60 fF to 20 fF. Figures II.2 and II.3 present the simulated results for R=4/20 ohms, respectively.

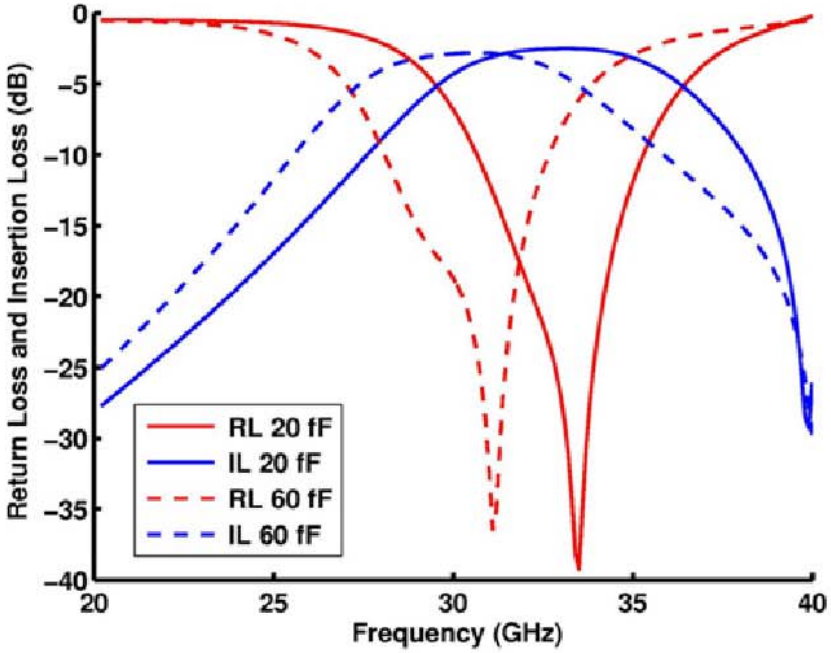

Figure II.2 – Simulated S parameters with R = 4 ohms.

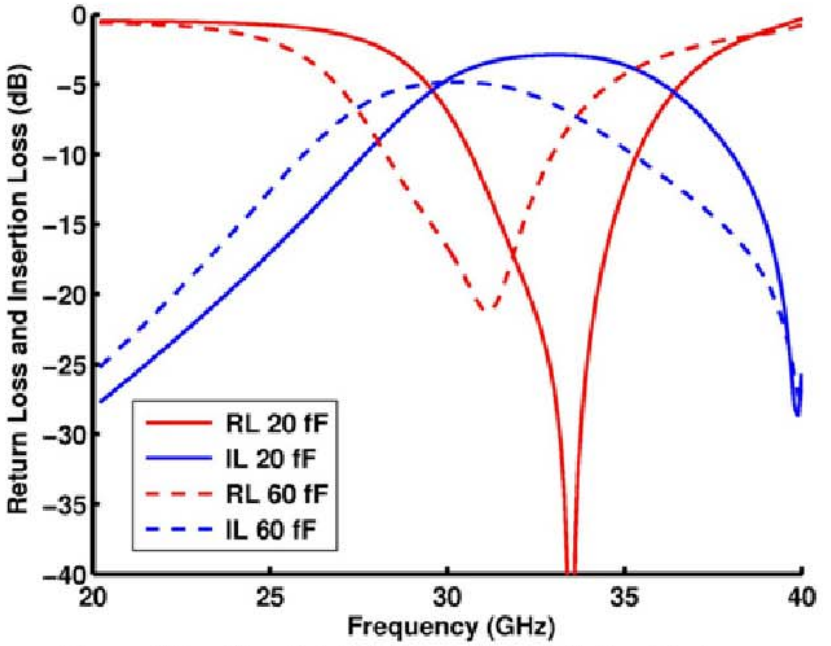

Figure II.3 – Simulated S parameters with R = 20 ohms.

In both cases, the center frequency tunes from 30.4 GHz up to 33 GHz, resulting in a tuning of 7.9%. The 3-dB fractional bandwidth is about 22-23%. When a series resistance of 4 ohms is assumed, insertion loss varies from only 2.83 dB to 2.5 dB from 30.4 to 33 GHz. Even assuming a high series resistance of 20 ohms, it will change from 4.85 dB to 2.91dB (from 30.4 to 33 GHz) which is very satisfying at these frequencies.

II. 2/ Measurements:

The filter is fabricated on a sapphire substrate with a similar process as the filter presented in Section I. The filter performance is measured after an SOLT calibration is performed. However, the response (insertion loss shape) did not look like expected due to a parasitic resonance (around 32 GHz). This resonance had been attributed to parasitic modes that can occur due to the specific coplanar feedline used in this design. In order to confirm this assumption and remove this parasitic effect, bonding wires had been added in order to create a bridge between the two ground planes, at the input and output, as shown in Figure II.4.

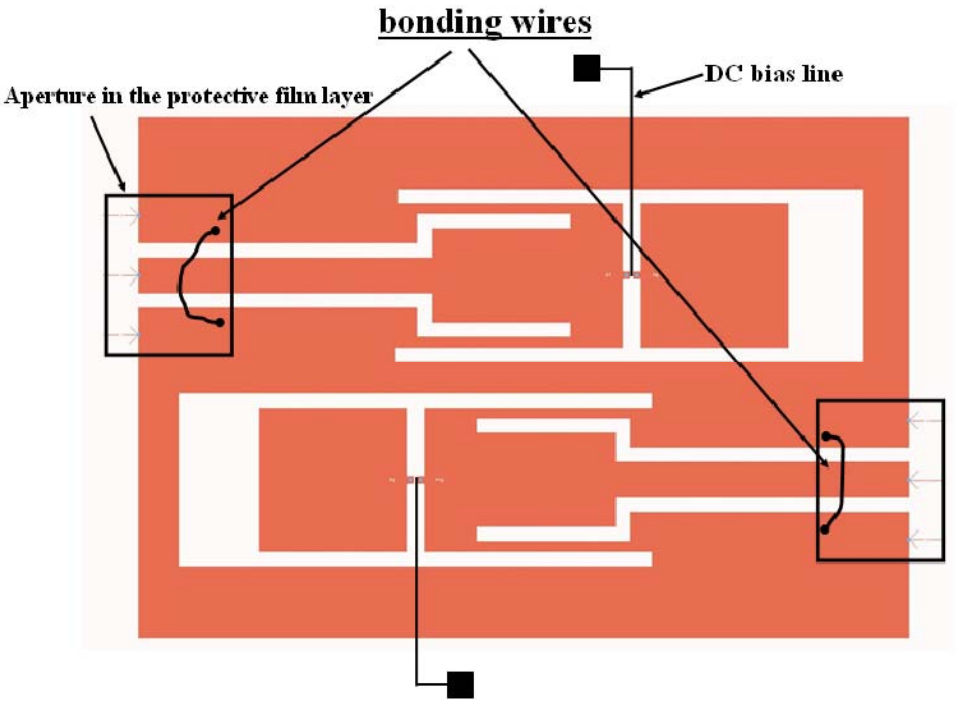

Figure II.4 – Layout of the filter with bonding wires at the input and output.

The use of bonding wires can remove the parasitic resonance. Figures II.5 and II.6 present the measured responses, without and with the bonding wires. Retro-simulations have been performed with both Momentum and HFSS, but none of these softwares were able to predict this effect. Figure II.7 and II.8 compares the simulated response to the measured one. Figure II.9 and II.10 present the simulated response with HFSS for C = 60 fF and C = 20 fF.

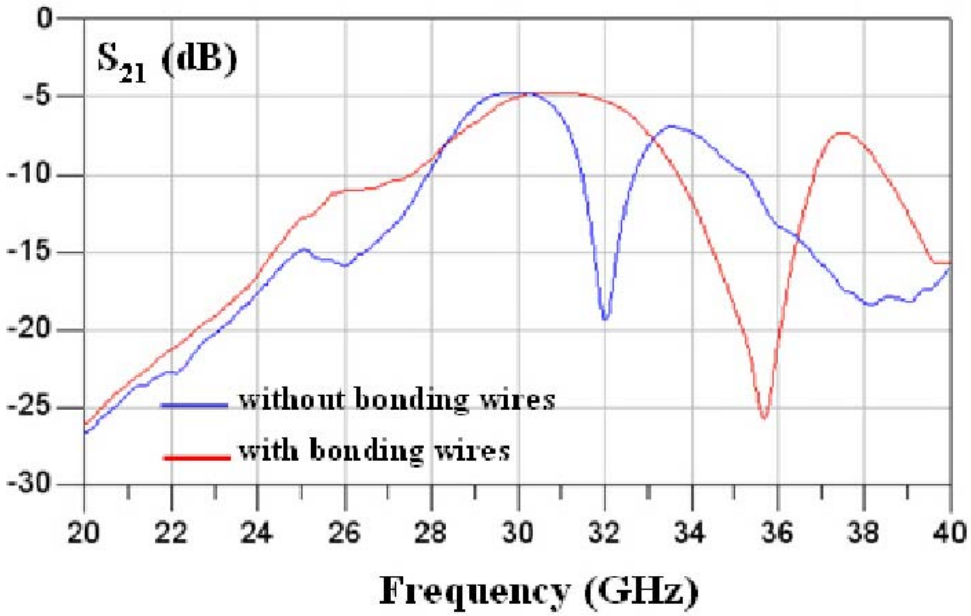

Figure II.5 – Measured insertion loss without and with bonding wires.

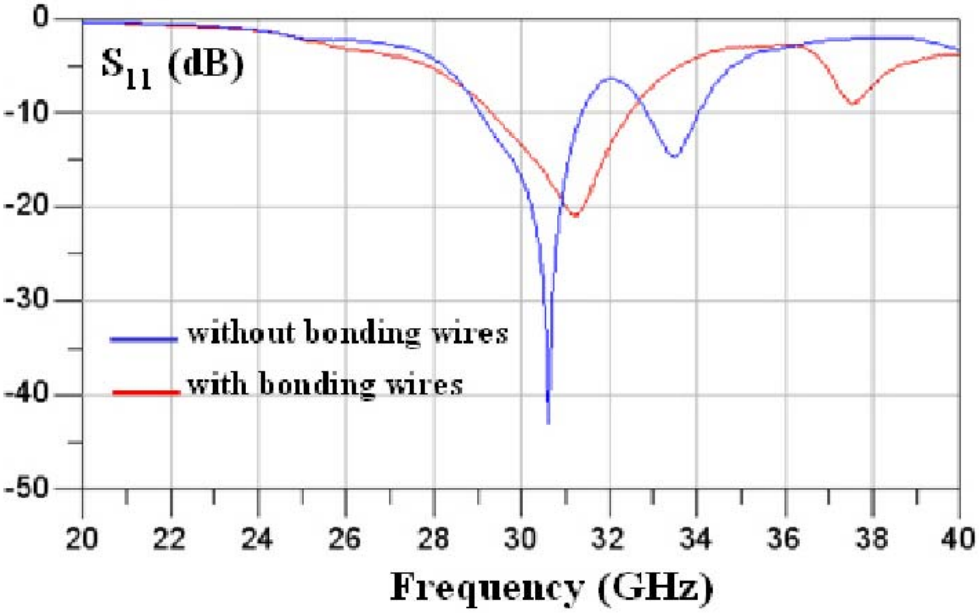

Figure II.6 – Measured return loss without and with bonding wires.

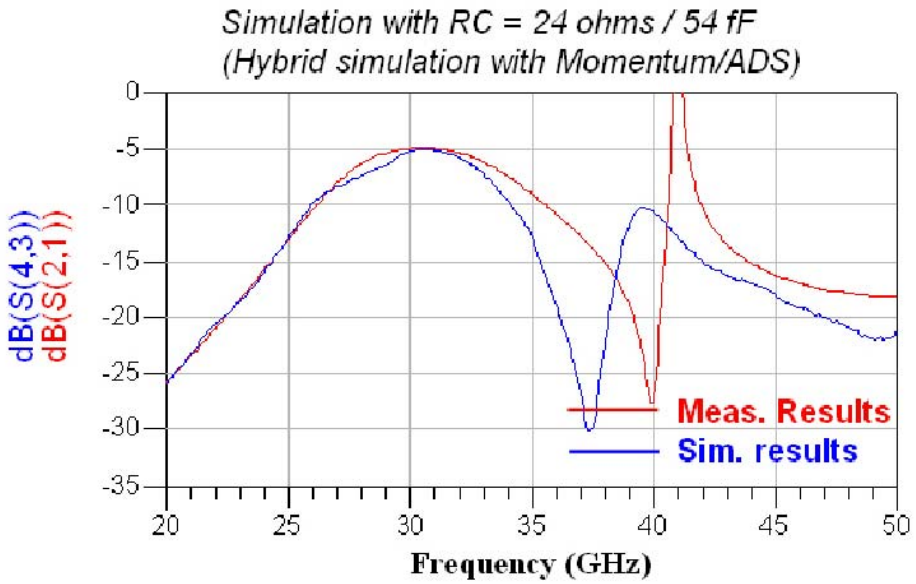

Figure II.7 – Measured insertion loss compared to the simulated response.

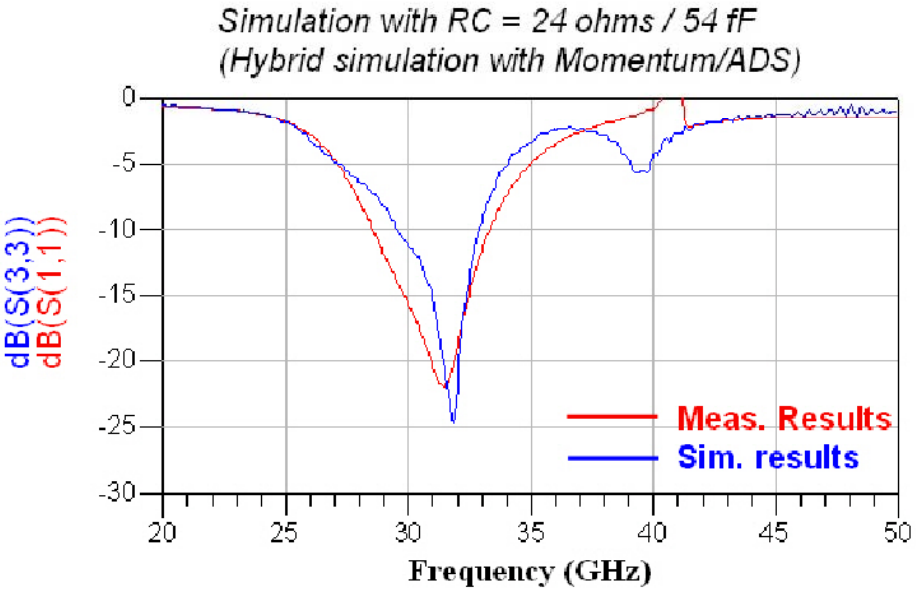

Figure II.8 – Measured return loss compared to the simulated response.

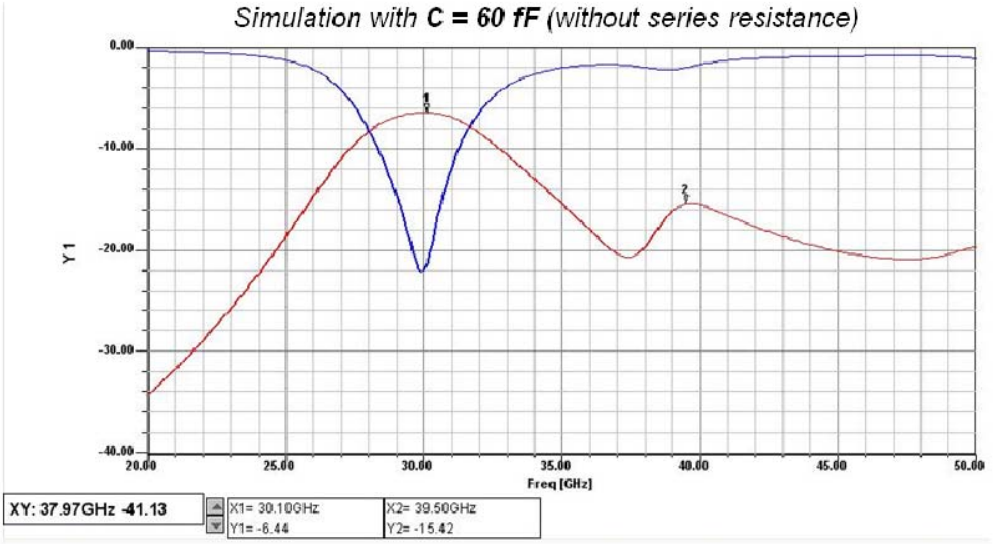

Figure II.9 – Simulated response with HFSS (C = 60 fF).

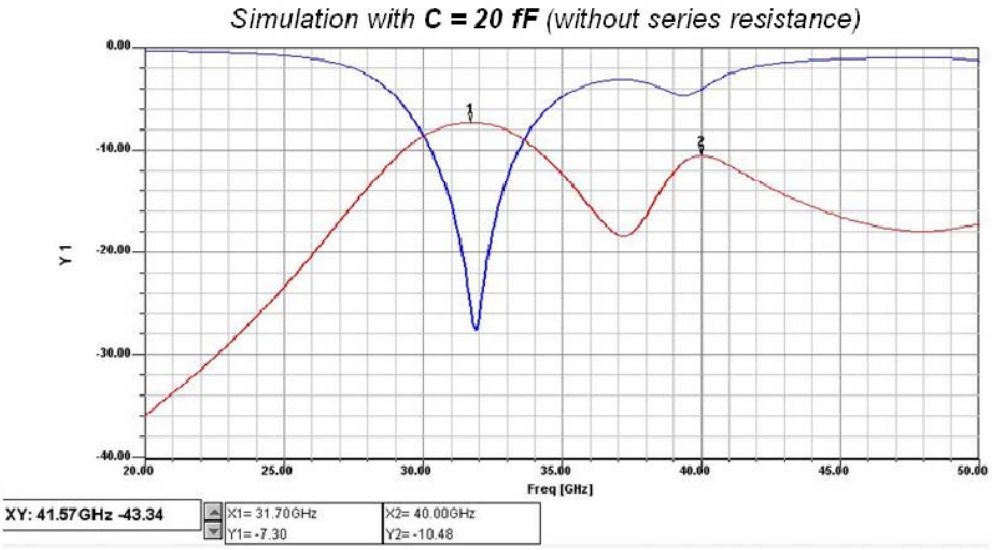

Figure II.10 – Simulated response with HFSS (C = 20 fF).

Several samples have been fabricated and tested. Two filters per sample are fabricated with 2 different biasing networks. However, it appears that for one of them, only one capacitor is working. Also, the film does not seem to handle a lot of voltage on this topology. It has been seen several times that the film broke out at only 10-20 V. When it tunes, the response does not seem to tune that much, especially the insertion loss. The tuning is very poor. This problem could be due to the quality of the film and the topology of the filter. A typical tuning achieved with the biasing of only one capacitor is presented in Figure II.11.

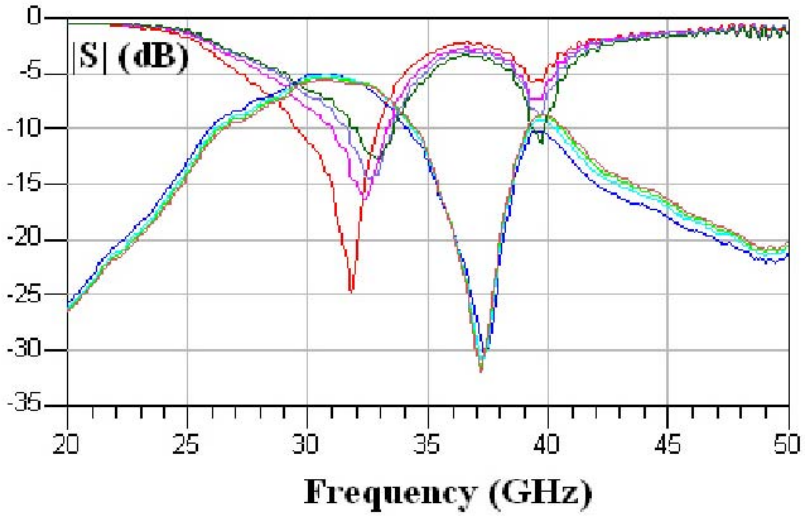

Figure II.11 – Example of "poor" tuning achieved by biasing one capacitor.

Part III

Tunable filter based on cross-coupled resonators

III. 1/ Filter design:

This Ka-band tunable bandpass filter is composed of four CPW cross-coupled quarter-wavelength resonators, which are loaded with BST thin film varactors located at the end of the resonators, as shown in Figure III.1.

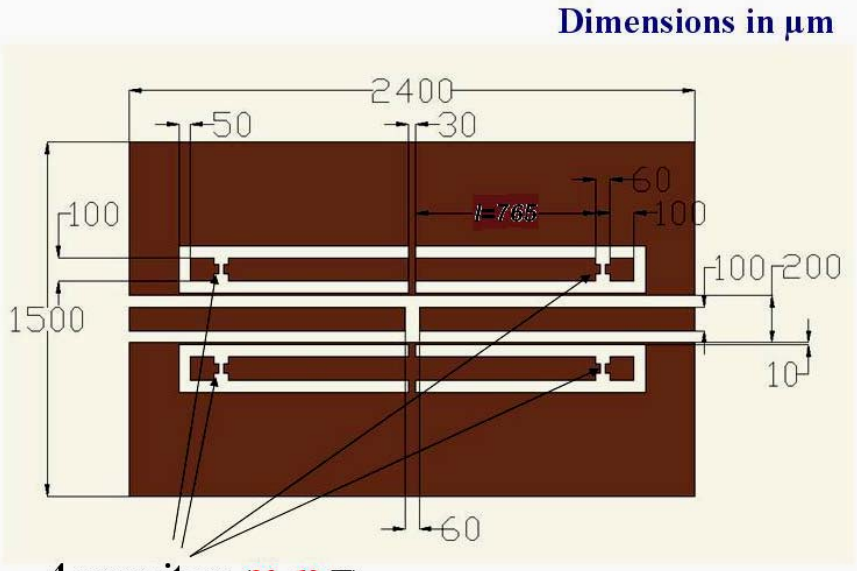

Figure III.1 – Cross-coupled resonators filter.

This structure shows a quasi-elliptical band pass function. It exhibits good performance including low insertion loss in its passband and high out-of-band rejection level in both lower and upper stopbands. Furthermore, there are also two transmission zeros in its stopband and their position may be controlled by adjusting the coupling between two resonators. By changing the value of the loaded BST thin film varactors, the electrical length of the resonators can be varied, and therefore the center frequency is tuned.

The whole circuit is designed on a 430-µm thick sapphire substrate (ε_r=10). The copper metallization of the filter is 2-µm thick. The tunable capacitors range from 60 fF to 20 fF, resulting in a ratio of 3:1.

III. 1/ Simulated results:

The dimensions of a filter with relative good performance were optimized. The key factor affecting the performance of this reconfigurable filter is the location of BST thin film varactors. Decreasing the distance *l* between the BST thin film varactors and the center ground line (Figure III.1) will increase the tuning, but worsen the insertion/return

loss, and vice-versa. The designed filter represents a trade-off between the tuning that can be achieved and the magnitude performance. The intrinsic loss of the BST thin film varactors, which can be represented by a series resistor *R*, is theoretically proportional to the frequency. Working in Ka-band, this other key factor must be considered. After optimization, when *l* = 765 μm and *R* = 4 ohms, the center frequency tunes from 33 to 34.4 GHz (4.2% tuning) when the capacitance value *C* varies from 60 to 20 fF. The 3-dB fractional bandwidth ranges from 8.8% to 9.3%. The insertion loss changes from 4.83 dB to 4.42 dB. The simulation results are shown in Figure III.2. When *R* is increased to 20 ohms, the insertion loss increases to 6.41 dB and 5.07 dB at 33 GHz and 34.4 GHz, respectively, as shown in Figure III.3.

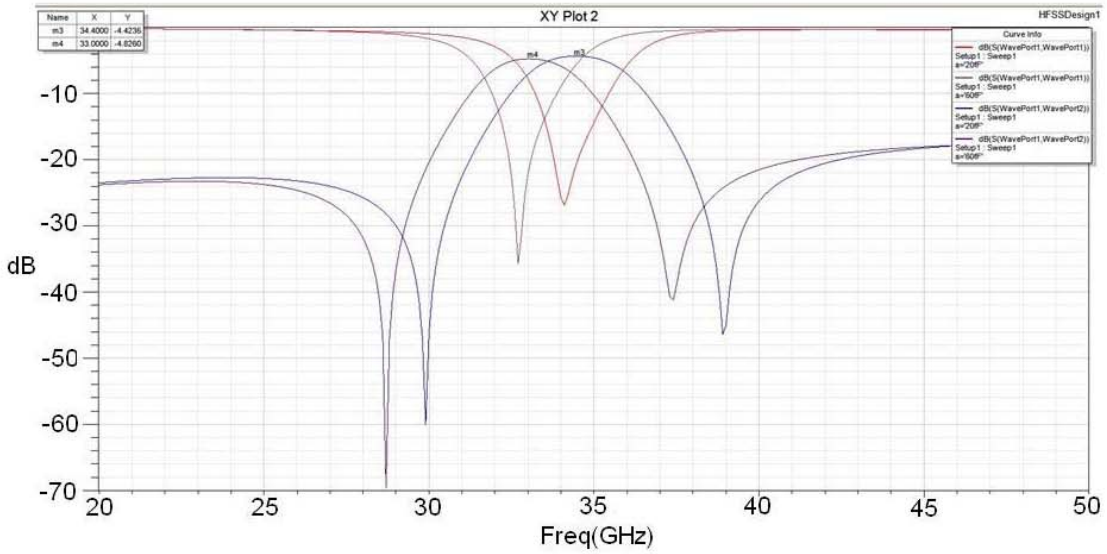

Figure III.2 – Simulated response with R = 4 ohms (l = 765 μm).

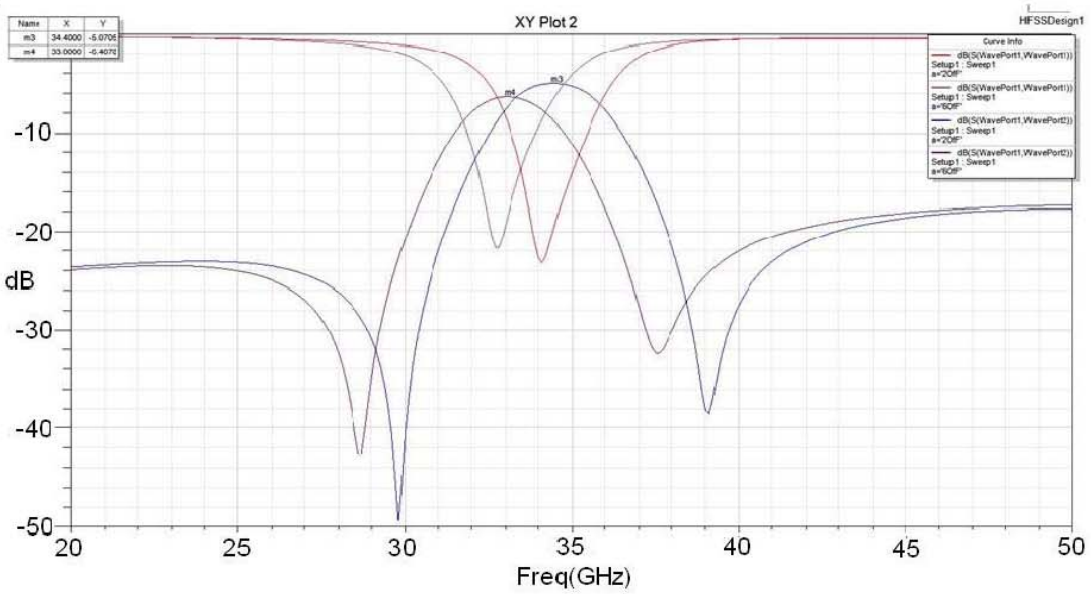

Figure III.3 – Simulated response with R = 20 ohms (l = 765 μm).

In order to get a better tuning, *l* can be modified. For *l* = 665μm and *R* = 4 ohms, the center frequency tunes from 33 to 36.9GHz, resulting in a tuning of 11.2%, when *C* changes from 60 to 20 fF, as shown in Figure III.4. The insertion loss is about 5.74 dB at 33 GHz and 4.61 dB at 36.9GHz. However, assuming a high series resistance of 20 ohms, the insertion loss deteriorates a lot: 10.1 dB at 33GHz and 6.04 dB at 36.9 GHz, as shown in Figure III.5.

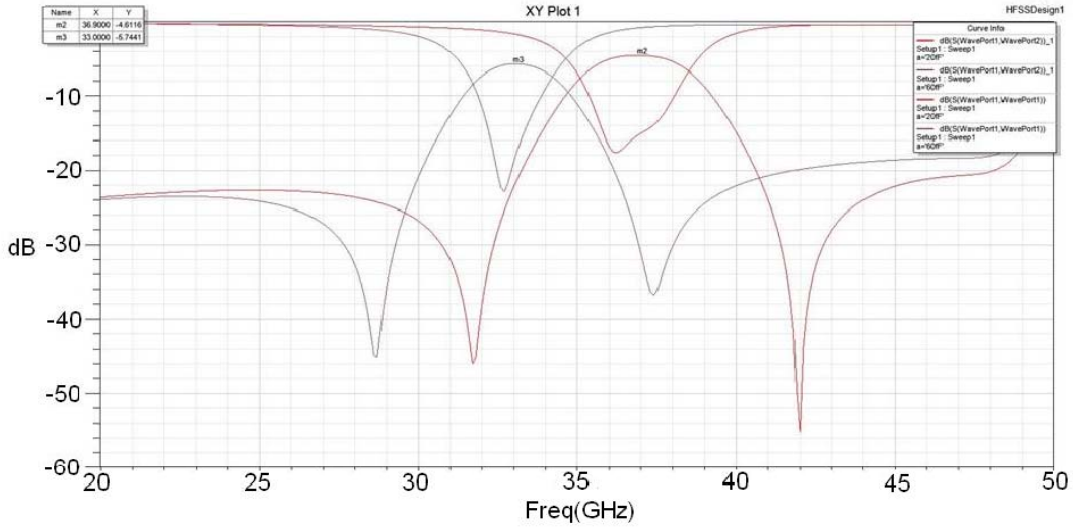

Figure III.4 – Simulated response with R = 4 ohms (l = 665 μm).

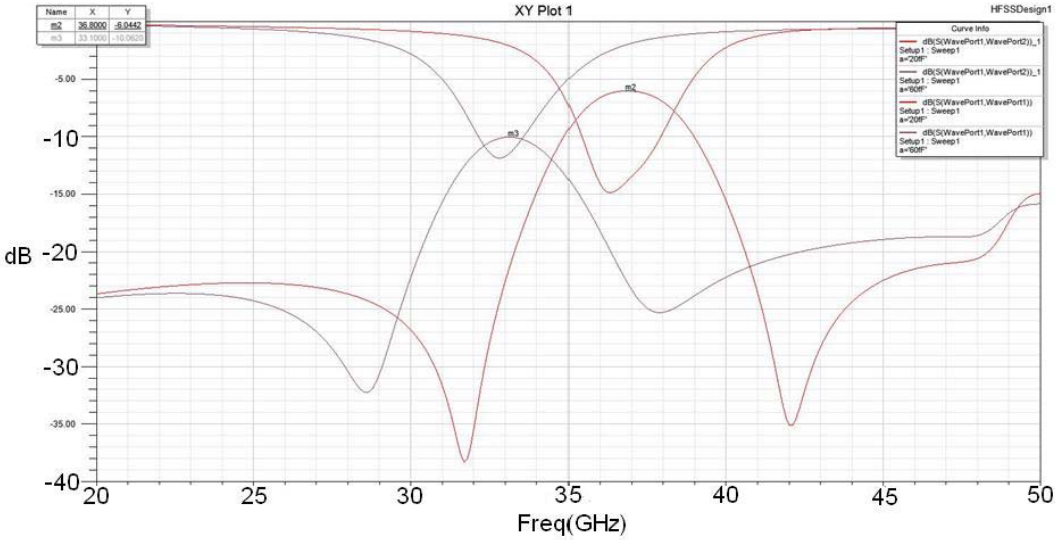

Figure III.5 – Simulated response with R = 20 ohms (l = 665 μm).

Part IV

Development of a tunable, folded-waveguide filter in the Ka-band

IV. 1/ Folded Waveguide: Principle of operation and Design:

The basic operation of a folded waveguide is extensively explained in [1] and in [2]. In a folded waveguide, the fundamental TE_{10} mode of a rectangular waveguide (Figure IV.1) is "folded" around the longitudinal axis running across the center of one of the sides indicated with dimension *2a* (Figure IV.1) of the waveguide. Therefore, the folding process reduces the footprint area of the filter by half as the longer side of the rectangular waveguide cross-section is reduced from *2a* to *a* (Figure IV.2). By providing a slot aperture of width *w* across the axis where the folding is performed, it is possible to properly develop the TE_{10} mode in a "folded" fashion, as shown in Figure IV.2.

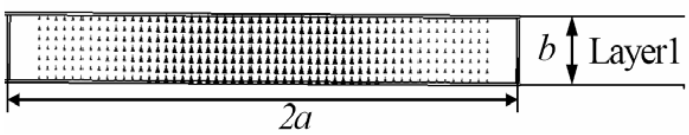

Figure IV.1 - Rectangular waveguide cross-section showing the electric field distribution of the TE_{10} mode (Fig. IV.1 from [2]).

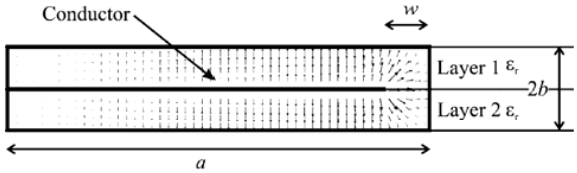

Figure IV.2 - Folded rectangular waveguide cross-section showing the electric field distribution for the "folded" TE_{10} mode (Fig. IV.2 from [1]).

In [1], designs rules are also presented to obtain the dimensions of the waveguide for folded operation. Fixing the substrate height (*b=430 μm*) and by using *b/a=0.4* (as suggested in [1]), we find that *a=1075 μm*. In addition, we see that *w/a=0.05* so the width of the slot that allows the folded operation is *a=53.75 μm*. Next, we proceed to verify whether the bandwidth of the folded waveguide is *not* less than the rectangular waveguide by verifying that $2w/a < b/a$, which for our case $0.1 < 0.4$ properly holds.

To verify that the design rules chosen correctly apply for our application and materials, we proceeded to simulate using HFSS [3] the folded waveguide using a sapphire substrate with $\varepsilon_r=10.0$. We see that the waveguide operation is substantially above the cut-off frequency as shown in the propagation constant plot in
Figure IV.3 (all distances simulated are above *a=1075 μm*).

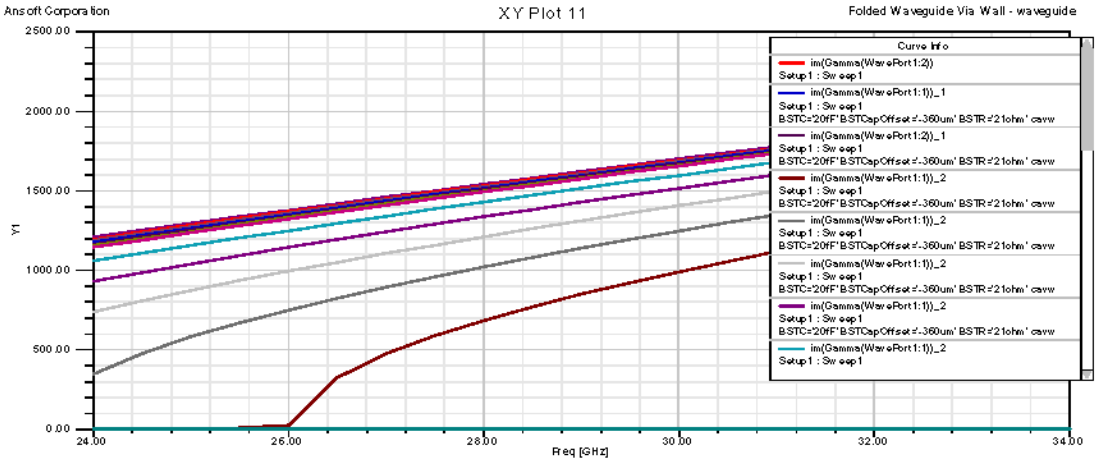

Figure IV.3 - Propagation constant plots showing the low cut-off frequency of the folded waveguide for different widths of the folded waveguide.

IV. 2/ Resonator design:

In this design two $\lambda_g/2$ (half the guided wavelength) resonators will be utilized to provide two poles in the pass band. An initial approximation of the $\lambda_g/2$ length is obtained with the Line Calculation tool available in [4] using a rectangular waveguide and then optimized in HFSS using a weak coupling. The low input/output coupling allows the determination a center frequency of about 32 GHz. From the optimized model we obtain that $\lambda_g/2=1500\ um$.

IV. 3/ The 2-pole filter realization:

After the $\lambda_g/2$ length has been chosen, the realization of the two-pole filter is performed by placing two $\lambda_g/2$ sections next to each other as done in [1]. Due to the high quality factor of the folded waveguide resonators, a weak coupling between the $\lambda_g/2$ sections is provided by extending and optimizing the length of the inter-resonator coupling section in the "Layout" layer shown in
Figure IV.4.a.

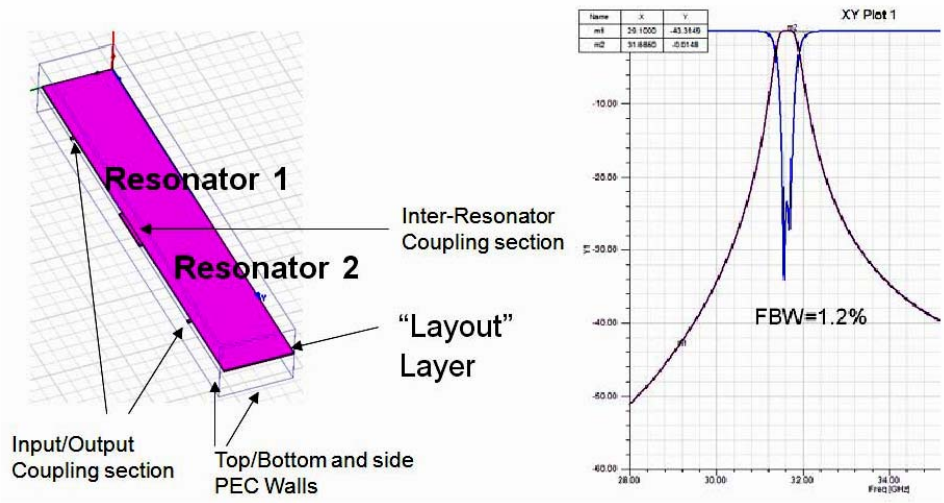

Figure IV.4 – (a) Ideal realization of the two-pole filter using two $\lambda_g/2$ sections, (b) Simulated S-parameter response of the folded waveguide filter with S_{11} in blue and S_{21} in maroon.

The input/output and inter-resonator coupling sections were optimized using HFSS to obtain the S-parameter response in
Figure IV.4b. A Perfect Electric Conductor (PEC) metallization was utilized to obtain the shown response.
Through the simulations we could observe that the lowest reflected signal level in the pass band (S_{11},
Figure IV.4.b) is achieved by shrinking as much as possible the length of the coupling section. Consequently, the level of S_{11} is limited by the minimum line width that can be patterned on the metallization layer of the circuit.

IV. 4/ Realization of the Vertical Walls of the Folded Waveguide:

Undoubtedly, the fabrication of the vertical walls of the folded waveguide has been the most challenging part of the implementation of the filter. An initial approach led us into the implementation of these walls using lines of via holes in a substrate-integrated waveguide arrangement (Figure IV.5) whose diameter and pitch was calculated according to [5].

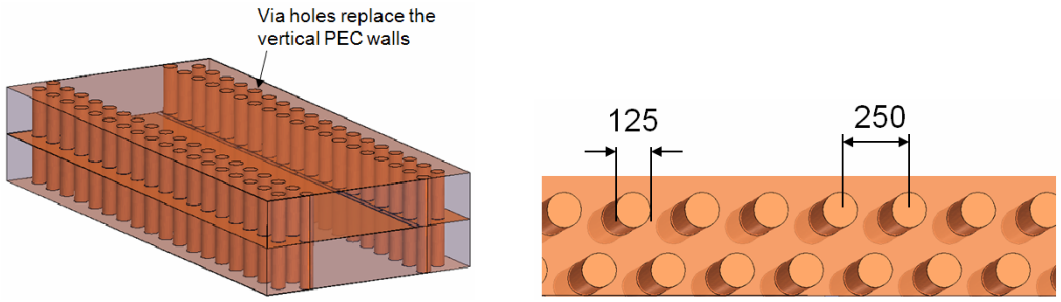

Figure IV.5 - (a) Folded waveguide filter modeled using vertical walls made of via holes in a substrate integrated waveguide fashion, (b) Dimensions of the via wall in µm.

Although simulations showed the successful operation of the filter with the substrate integrated waveguide arrangement, the perforation of such small holes and tight pitch proved to be extremely unfeasible for fabrication. Resonetics LLC (http://www.resonetics.com/), a company that specializes in laser micro machining offered to make perforations for three circuit samples for about $1,950.00 per day of work. However, the company recently communicated to us that they have re-oriented their operation for strictly commercial, large-scale projects which leaves small research projects, such as this project, outside their scope. Other companies have been contacted as well, but none of them have the capability to perform the drilling with such dimensions. Nonetheless, from the design stages it was assumed that the holes would be drilled by Resonetics, so the filter was optimized assuming via-hole walls with the dimensions shown in Figure IV.5.

IV. 5/ Frequency Tuning:

As mentioned previously, frequency tuning is achieved through BST tunable capacitors as demonstrated in [6]. In it is shown [7] that to achieve maximum tuning it is necessary to place the tuning element (in our case the BST capacitor), in the region within each resonating structure where the electric field has maximum intensity. By plotting the electric field distribution in HFSS we can observe that this region is located in the waveguide *slot side* at the middle of each resonator. Thus placing the BST capacitors in the vicinity of region causes the "ideal" tuning presented in Figure IV.7.

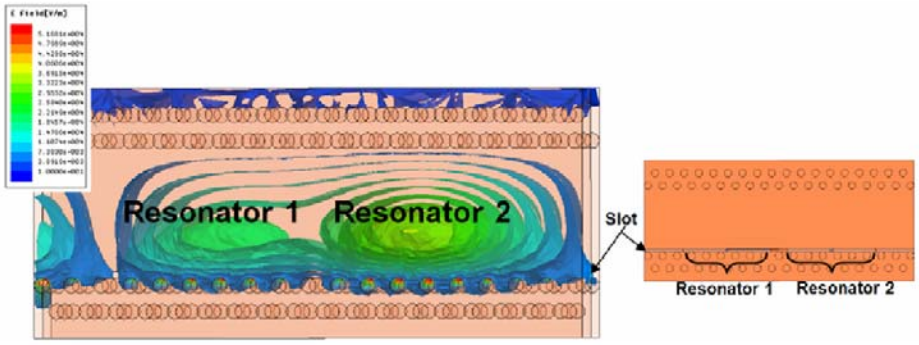

Figure IV.6 - Intensity distribution of the electric field within resonators 1 and 2 of the two-pole folded waveguide filter (top view).

For our simulations in HFSS, the BST capacitors have been modeled as two lumped element sheets: one capacitive and one resistive going from the layout layer (indicated in figure in
Figure IV.4a) towards the vertical walls of the waveguide (ground potential). We can also observe that ideal the insertion loss (IL) has increased to 1.88 dB assuming a resistor value of 1 Ω.

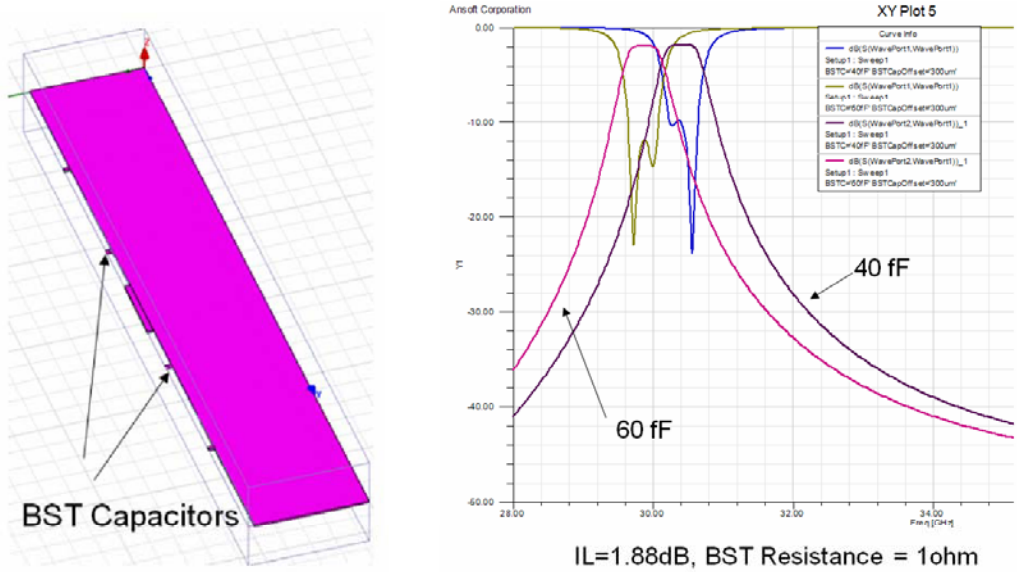

Figure IV.7 - Two-pole folded waveguide filter with tuning provided by BST capacitors: (a) Ideal model with PEC walls showing BST capacitor placement, (b) Simulated S-parameter response for two capacitance values.

Although placing the tuning element in the region of maximum electric field intensity causes maximum tuning, the fact that our BST capacitors have a significant resistive component has the added disadvantage of causing maximum insertion loss. Thus, a trade-

off is identified in the process of finding the optimal position of the BST capacitor along the folded waveguide slot: insertion loss versus tuning range.

By symmetrically sweeping the position of the capacitors along the slot of the folded waveguide, we see that a 10% tuning and a worse case 5 dB insertion loss is achieved by placing each capacitor at 756 µm from the inter-resonator coupling section. This optimization was performed taking into account the losses introduced by the copper metallization and by an assumed BST capacitor resistance of 10 Ω. A model was also simulated using only one line of via holes to test the effect of the via wall on the insertion loss. Both results are presented in Figure IV.8. A summary of the dimensions of the main features folded waveguide filter is presented in
Figure IV.9.

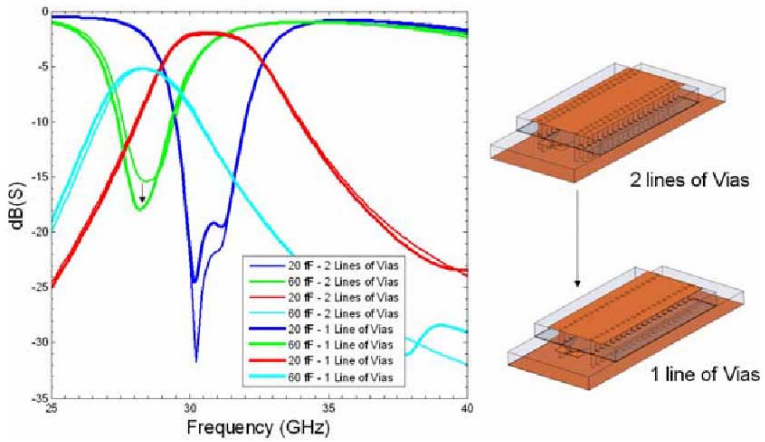

Figure IV.8 - Simulated S-parameter response of the substrate-integrated, folded-waveguide, two-poles filter using one and two lines of via holes as vertical walls.

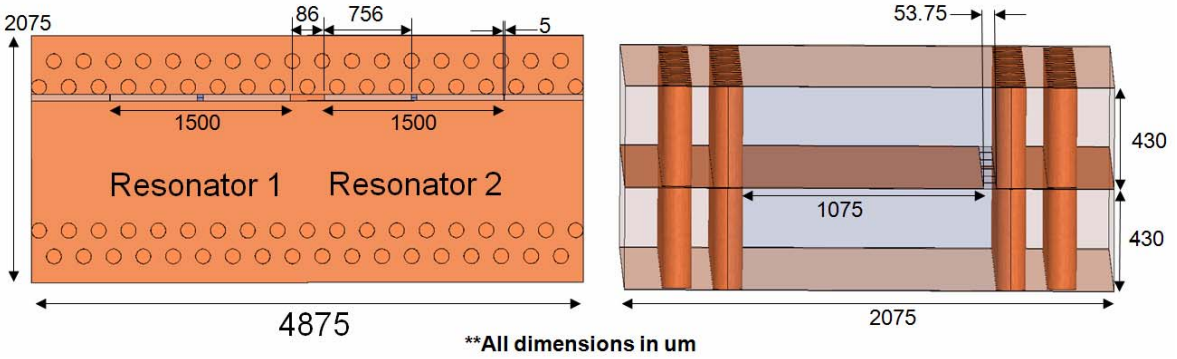

Figure IV.9 - Summary of the optimized dimensions of the two-pole substrate integrated folded waveguide filter in µm.

IV/ 6/ Filter Fabrication:

The fabrication of the folded waveguide filter is performed in a number of stages. First "layout" layer is patterned on the "bottom" sapphire substrate and a layer of cyclotene is applied to provide access to the bias circuitry. Three circuits are patterned in a 10 mm x 10 mm wafer as shown in Figure IV.10.

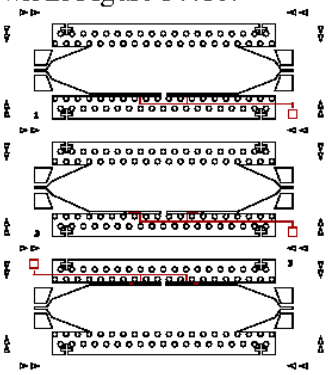

Figure IV.10 - Layout metallization layer patterned on the bottom sapphire layer with BST capacitor lines are shown in red.

Preliminary measurements were performed at this stage of the fabrication to verify the operation of the BST capacitors. Although it is difficult to interpret the measured data, a simulation was performed to study the measured response. The results slight change in the S-parameter response after varying the bias voltage from 0 V to 30 V. A comparison between the measurements and the simulated data (varying the capacitance value from 30 fF to 60 fF) are shown in Figure IV.11.

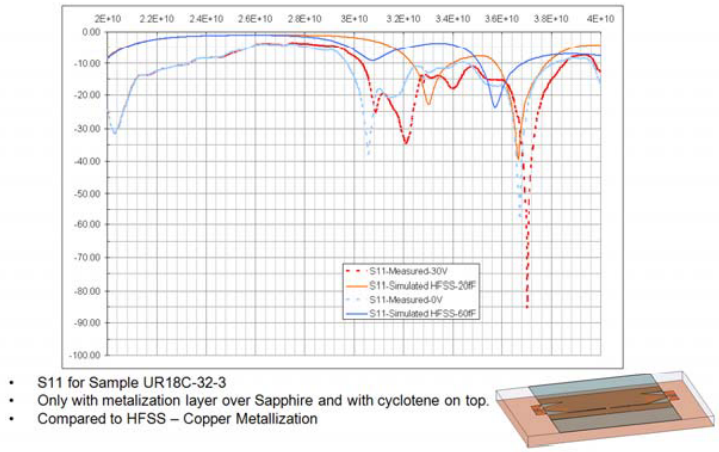

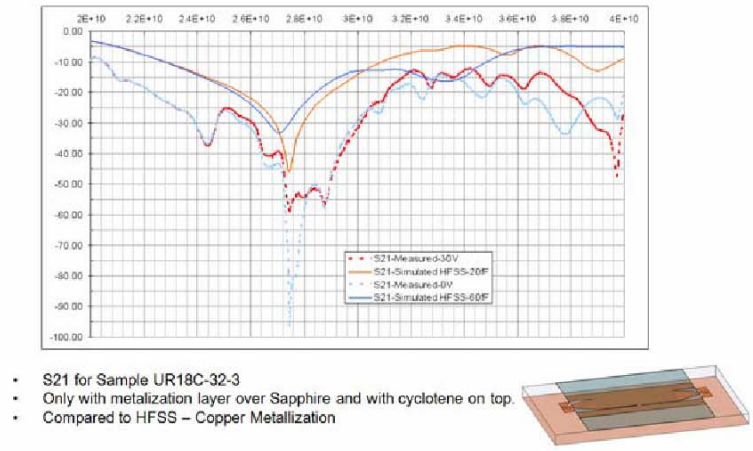

Figure IV.11: Simulated and measured S-parameter response of the metallized bottom sapphire layer.

After the "layout" metallization patterned on the bottom sapphire, the top layer is diced and bonded to the cyclotene using the Rogers 3001 bonding film. First, the bonding layer is cut using a CO_2 laser system to provide the best accuracy. Then, the bonding is achieved by using a Finetech sub-micron flip-chip bonder. The final substrate stack-up is shown in

Figure IV.12.

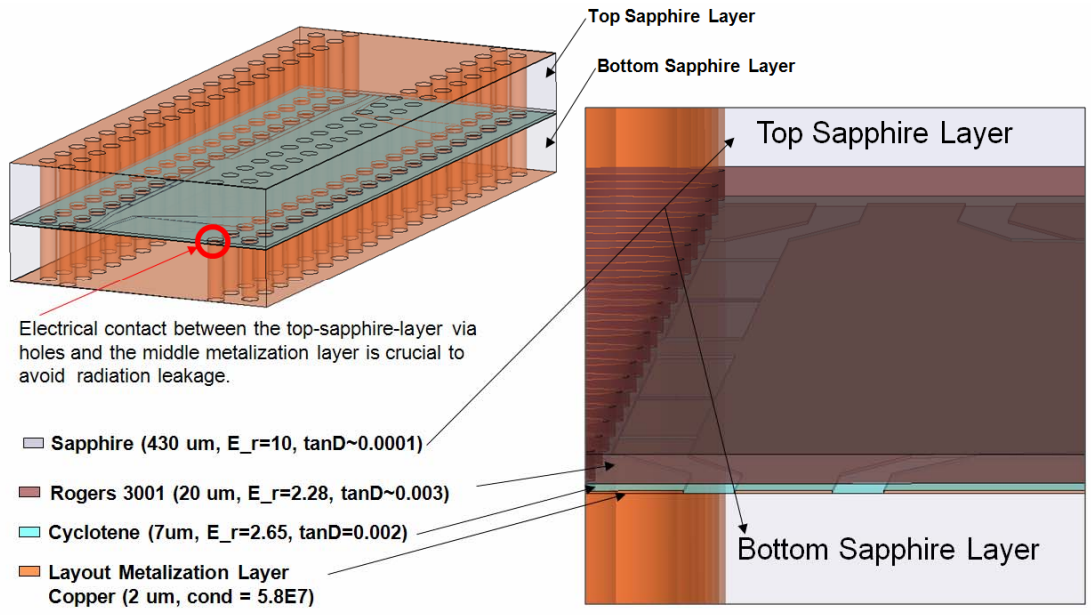

Figure IV.12 - Substrate stack-up of the folded-waveguide tunable filter.

Preliminary bonding results performed on dummy samples are shown in Figure IV.13. The estimated misalignment is of about 5-10 µm. This misalignment is caused by the large size of the sample in comparison with the limited movement of the camera used by the alignment system. Another possible source of misalignment is that the alignment marks are seen through the cyclotene in the bottom sapphire layer, which makes it difficult to properly focus the layer for bonding.

Figure IV.13 - Alignment result of bonding the top and bottom sapphire substrate layers (both layers have metallized alignment marks on the bonding side).

IV. 7/ Current status and future work:

Current efforts are focusing in improving the alignment technique for bonding prior to dicing of the individual filters. In addition, studies have been performed to create the vertical walls using solid copper metallization after dicing the samples. With solid vertical walls placed as close as 50 µm to the filter, the simulated filter response is shown in

Figure IV.14. Observe how walls placed at 50 µm from the layout area do not leave room for the BST capacitors bias line in the position it is currently patterned in the fabricated samples.

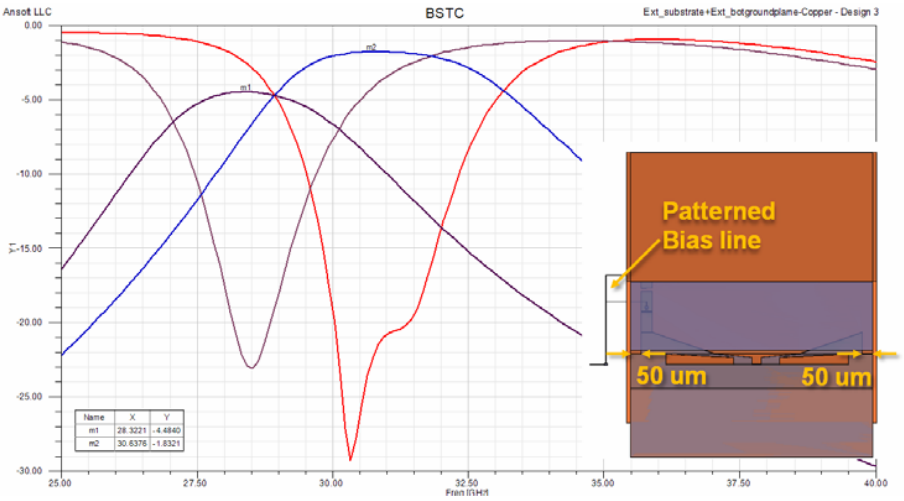

Figure IV.14 - Simulated S-parameter response of the folded waveguide tunable filter using solid copper for the vertical walls.

Consequently, fabricating vertical walls at 50 µm from the layout area would require a new fabrication or a test with un-biased BST capacitors. Another option to allow a test to show tenability would be achieved by providing room for the bias line by extending the distance to the via-wall. However, the filter response would significantly as observed in Figure IV.15.

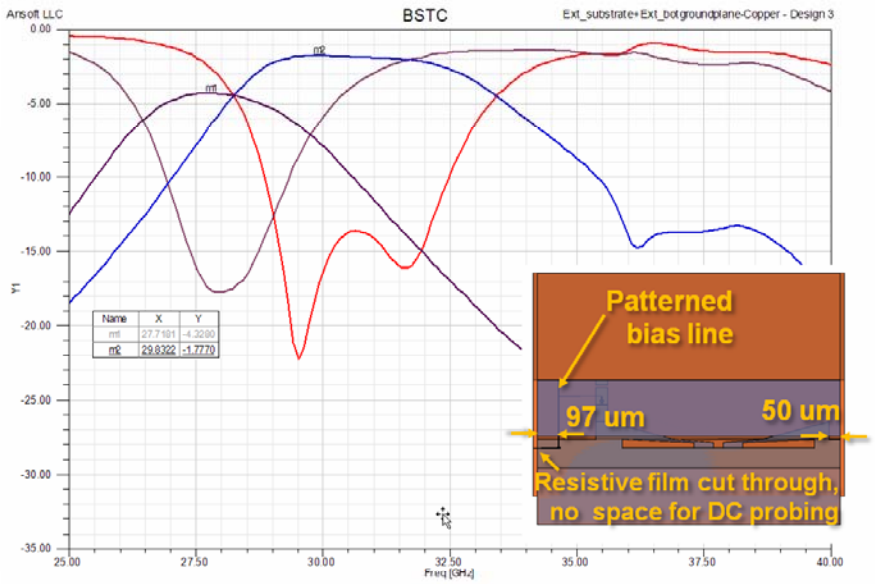

Figure IV.15 - Simulated S-parameter response of the tunable folded waveguide filter extending the distance between the layout area and the vertical wall.

References

[1] N. Grigoropoulos, B. Sanz-Izquierdo, and P. R. Young, "Substrate integrated folded waveguides (SIFW) and filters", *IEEE Micro. and Wireless Comp. Letters*, vol. 15, no. 12, pp. 829–831, 2005.

[2] G. H. Zhai, W. Hong, K. Wu, J. X. Chen, P. Chen, and H. J. Tang, "Substrate integrated folded waveguide (SIFW) narrow-wall directional coupler," in *Proc. Int. Conf. Microwave and Millimeter Wave Technology ICMMT 2008*, vol. 1, 2008, pp. 174–177.

[3] "High Frequency Structure Simulator (HFSS)," Ansoft LLC, 2009, version 12.0.1.

[4] M. Margraf, S. Jahn, and J. Flucke, "Quite universal circuit simulator (QUCS)," Available Online at http://qucs.sourceforge.net/, September 2009, version 0.0.15.

[5] K. Wu, D. Deslandes, and Y. Cassivi, "The substrate integrated circuits - a new concept for high-frequency electronics and optoelectronics," in *Proc. 6th Int. Conf. Telecommunications in Modern Satellite, Cable and Broadcasting Service TELSIKS 2003*, vol. 1, 2003.

[6] S. Courrèges, Y. Li, Z. Zhao, K. Choi, A. Hunt, and J. Papapolymerou, "Ferroelectric tunable bandpass filters for Ka-band applications," in *Proc. 38th European Microwave Conf. EuMC 2008*, 2008, pp. 55–58.

[7] A. L. Amadjikpe and J. Papapolymerou, "A high-Q electronically tunable evanescent-mode double-ridged rectangular waveguide resonator," in *Proc. IEEE MTT-S Int. Microwave Symp. Digest*, 2008, pp. 1019–1022.

Conclusions:

This report has demonstrated the design and simulations of BST-based tunable bandpass filters that operate in Ka-band.

In the first section, a 3-pole filter is presented. The filter is built on sapphire and uses a coplanar topology. At the highest center frequency, the filter exhibits insertion loss of only 2.5 dB. The maximum bias voltage for the BST is only 30 V. The center frequency tunes from 29 GHz to 34 GHz.

The second section of the report presents a 2-pole filter, also using a coplanar topology. Here, the electrical length of the two resonators can be changed by biasing the BST capacitors, resulting in the tuning of the center frequency. Issues regarding the fabrication have been discussed.

The third section deals with another CPW Ka-band filter. In that case, cross-coupled resonators are used and 4 BST capacitors that are located at the ends of each resonator in order to make the center frequency of the filter tune. The length of the resonators can be adjusted in order to get a better tuning or better performance.

The final section shows the design of a 2-pole tunable folded waveguide filter. The center frequency of this filter can tune from 27.72 GHz to 30.50 GHz. This topology allows a reduction size of 50% compared to standard waveguide filters.

Publications

S. Courrèges, Y. Li, Z. Zhao, K. Choi, A. Hunt, S. Horst, J. D. Cressler, and J. Papapolymerou, "A Ka-Band Electronically Tunable Ferroelectric Filter", *IEEE Micro. and Wireless Comp. Letters*, vol. 19, no. 6, pp. 356-358, 2009.

S. Courrèges, Y. Li, Z. Zhao, K. Choi, A. Hunt, and J. Papapolymerou, "Ferroelectric tunable bandpass filters for Ka-band applications," in *Proc. 38th European Microwave Conf. EuMC 2008*, 2008, pp. 55–58.

4. Commercialization

A special aspect of SBIR programs is to help transition technology to commercial practice. This effort helped move nGimat tunable dielectric capability towards commercialization. We reduced loss and reduced the size of parts. This is very important to commercial applications. We presented results at a couple of conferences and published results with Georgia Tech.

The best commercialization at the current time is for phase shifters with Power Wave. The reduced loss and equipment repairs in part funded by this SBIR helped moved this closer to occurring. We are near a possible order for 200,000 parts, with more follow-on orders after this. We will continue

on commercial capability after this effort. Any part sales from our tunable dielectrics will help other part types (phase shifter sales will help future tunable filter sales).

5. Conclusions

As a summary, in this reporting period, BST thin films with different compositions were deposited on *c*-sapphire substrates. After comparing the tuning, insertion loss and figure of merit of all of these samples, we selected one of the composition for 2" inch wafer BST deposition. Electrode processing equipment was made functional and tested. Four Ka-band devices were fabricated from two different wafers having different thickness using nGimat and Gatech design structures. The measured S-parameters for return loss and insertion loss are reported also.

We deposited two different dual layer BST samples for temperature stable study. The variation of capacitance vs temperature of one of the samples is as small as 2 % in the entire temperature range under a bias of 16 V voltage. This composition is promising for future temperature stable RF device applications. We have a commercial application for which we are hoping to make many phase shifters with this composition.

We still have the problem to get repeatable tuning BZN thin films. BZN thin films show very small insertion loss (<1dB to 2dB) in a range of 0 to 67 GHz. Although sometimes we can get tunable BZN films, it is not repeatable. We will continue to do more extensive research on BZN thin film deposition.

We are still working on the device fabrication of Ka-band Substrate-Integrated Folded-Waveguide (SIFW) Filter designed by Gatech. We will submit the results in the future to the TPOC once we finish the fabrication and measurements.

6. Equipment Used

- CCVD
- Class 100 cleanroom
- Complete microlithography equipment set
- Hitachi S-800 Field Emission Scanning Electron Microscope (SEM)
- Siemens General Area Detector Diffraction System (GADDS)
- Agilent Vector Network Analyzer 8510 or PNA 8353
- LCR Meter

7. Personnel

Personnel	**Responsibility**
Yongqiang Wang, Ph.D. –Research Engineer, and Principal Investigator	Fabrication and oversees project, materials development
Andrew Hunt, Ph.D. – CEO/CTO	Supervisor
Kwang Choi, Ph.D. – RF Engineer	Design and testing
Deepika Rajamani – Process Engineer	Deposition, evaporation
John Papapolymerou, Ph.D. – Subcontractor	Filter design and RF measurements

8. Percentage of Each Task Completed

Phase II Task	**Task Completed**
1. Improve BST	100%
2. BST Temperature Stability	100%
3. Improve Filter Design	100%
4. Deposit BZN	100%
5. Fabrication/Testing	90%
6. Optimize Ferrite Films	60%
7. Ferrite Filters	35%
8. Prototyping	90%
9. Scale-up	80%
10. Customer Relations	70%
11. Report	100%